UPPSALA
UNIVERSITET

UPTEC X 17 023
Examensarbete 30 hp
September 2017

Targeting HSP90 with the inhibitor AT13387 in tumour cells

Martina Nilsson

UPPSALA
UNIVERSITET

Teknisk- naturvetenskaplig fakultet
UTH-enheten

Besöksadress:
Ångströmlaboratoriet
Lägerhyddsvägen 1
Hus 4, Plan 0

Postadress:
Box 536
751 21 Uppsala

Telefon:
018 – 471 30 03

Telefax:
018 – 471 30 00

Hemsida:
http://www.teknat.uu.se/student

Abstract

Targeting HSP90 with the inhibitor AT13387 in tumour cells

Martina Nilsson

The use of HSP90 inhibitors as drugs for cancer has been under research for a long time. The synthetic made inhibitor, AT13387 is one of them. AT13387 is in clinical trials and is looking promising as a therapeutic drug for cancer. However, since cancer cells can be radioresistant researchers are focusing on finding radiosensitizing agents. Previous publications show that AT13387 might be one of these radiosensitizing agents. This study is investigating whether AT13387 possesses radiosensitizing effects on tumour cells and what the mechanisms behind this radiosensitizing effect can be. Results from this study are showing trends of radiosensitizing effects on tumour cells although more investigation is needed. The study reveals up- and down regulation of several important proteins in tumour cells after treatment with the drug and irradiation. It also demonstrates the effect the treatment has on cell viability and migration. This study supports the fact that AT13387 is a promising therapeutic drug against cancer and promotes more investigation in the co-treatment of AT13387 and irradiation.

Handledare: Diana Spiegelberg
Ämnesgranskare: Marika Nestor
Examinator: Jan Andersson
ISSN: 1401-2138, UPTEC X 17 023

Targeting HSP90 with the inhibitor AT13387 in tumour cells

Martina Nilsson

Populärvetenskaplig sammanfattning

Cancer är en världssjukdom som tar allt för många liv. Den kommer i många olika varianter och forskare gör sitt yttersta för att utveckla den bästa behandlingen. Det faktum att världsbefolkningen ökar snabbt i takt och att utvecklingsländer blir rikare gör att fler fall av cancer kommer upptäckas per år många år framöver. Vi lever idag i en värld där många ohälsosamma beslut tas och risken för att utveckla cancer är i många fall stor. Cancer är en sjukdom som de flesta av oss kommer att stöta på någon gång under vår livstid, antingen blir vi själva drabbade eller en anhörig.

Många i forskningsvälden idag fokuserar på att patienter ska få en mer individuell behandling av sin cancer för att behandlingen ska bli så effektiv som möjlig. Det gäller att hitta lämpliga markörer i cancercellerna för att på bästa sätt vinna över cancern. Idag så finns det många olika behandlingssätt mot cancer, en av de kanske mest använda och framgångsrika är strålning. Dock är det inte ovanligt att många cancerceller är resistenta mot strålning och därför är kombinationen av strålning tillsammans med en produkt som gör cellerna strålningskänsliga önskvärd. En sådan produkt är möjligtvis AT13387, en syntetisk inhibitor som har kommit en bit på väg till att förhoppningsvis bli en framgångsrik medicin mot cancer. AT13387 inhiberar ett överuttryckt protein, HSP90, i cancerceller. Detta har visat sig vara mycket framgångsrikt då HSP90 kontrollerar många cancerogena proteiner i cellerna. Idag är AT13387 ute i kliniska prövningar, dock ej tillsammans med strålning. Det finns publikationer som tyder på att AT13387 besitter strålningskänsliga egenskaper och därför är intressant att undersöka mer.

Syftet med detta projekt var att undersöka och karakterisera AT13387 tillsammans med strålning på mänskliga tumörceller med förhoppningen att kunna förklara mekanismen bakom AT13387s strålkänsliggörande egenskaper. För att nå detta mål har olika experiment och analyser utförts.

Examensarbete 30 hp

Civilingenjörsprogrammet i molekylär bioteknik

Uppsala universitet, september 2017

Table of contents

Abbreviations

ADP – adenosine diphosphate

ATP – adenosine triphosphate

BSA – bovine serum albumin

CCD camera – charge-coupled device camera

DMSO – dimethyl sulfoxide

EDTA – ethylenediaminetetraacetic acid

EGFR – epidermal growth factor receptor

ER – endoplasmic reticulum

FCS – fetal calf serum

HER2 – human epidermal growth factor receptor 2

HSP70 – heat shock protein 70

HSP90 – heat shock protein 90

L-glut – L-glutamine

PBS – phosphate buffered saline

PBS-T – phosphate buffered saline with Tween-20

Pest – penicillin-streptomycin

PVDF – polyvinylidene difluoride

VEGF – vascular endothelial growth factor

VEGFR – vascular endothelial growth factor receptor

53BP1 – p53 binding protein 1

1 Introduction

It is nothing new that cancer is one of the leading causes of death worldwide. In 2012, 14.1 million new cases of cancer were detected and 8.2 million deaths occurred due to cancer across the globe (Torre *et al.* 2015). Even though there is a lot of research going on in this field and treatments are getting better, cancer is an enormous burden to the society. The fact that we are getting older and that the population is increasing is not making it any easier to overcome the disease. According to Torre *et al.* (2015) the high rate in which these two factors are increasing, especially in developing countries, is making cancer still going to be one of the leading causes of death for years to come. Even though people's knowledge regarding the risks of developing cancer from smoking, drinking too much alcohol, no physical activity and poor diet has increased, people all around the world are still taking these risks.

In men, the most common cancer types are lung, prostate and colorectal cancer and in women, breast and colorectal cancer are the leading types (Jemal *et al*. 2010). Despite all the research and improvements that are being done in cancer treatment according to Jemal *et al.* (2010) cancer is still taking more lives than heart diseases in people younger than 85 years. It is therefore of great importance that more research is being done in this complex world of cancer.

Today there are different options when it comes to treating cancer. It all depends on which type of cancer the patient has, in what stage the cancer is in and what health status the patient has. The treatments vary from surgery, chemotherapy, radiotherapy, immunotherapy etc. The options are many. Many times a co-treatment is the best strategy to defeat the disease. (National cancer institute, 2017)

A major focus in the world of cancer research today is to achieve a more personalized treatment. This has become possible due to the fact that in the two last decades there has been a rapid growth in genomic and proteomic data (Phan *et al.* 2009). Being able to understand molecular mechanisms in the body will give us a better understanding on how diseases work and how we can tailor each treatment for each individual. The understanding of a disease, for example cancer, will be easier if we learn to recognize different biomarkers. A biomarker can for instance be a mutant gene, RNA, proteins or small metabolite molecules. A biomarker is a marker that is specific for a certain disease. This recognition of a biomarker can be of great help for a more personalized treatment. For instance, Phan *et al.* (2009) describes how the recognition of the protein HER2 in patients with breast cancer tells the physician which specific treatment this patient would benefit from.

A successful and very common therapy is radiotherapy. Although it is successful and developed it can still get better in terms of selectivity and efficacy. In many cancer types radioresistant cells get selected (Kabakov *et al.* 2010). Therefore, Kabakov *et al.* (2010)

suggests that a co-treatment with a radiosensitizing agent together with radiotherapy is an attractive solution. This would lower the radiation dose for patients and therefore be a better treatment choice.

1.1 Background

1.1.1 HSP90

Heat shock protein 90, HSP90, is a chaperone protein that is commonly abundant within all cells (Whitesell & Lindquist, 2005). In fact, 1-2 % of the whole proteome are HSP90 proteins according to Whitesell & Lindquist (2005). They came to the conclusion that this amount will increase up to a two-fold when the cell is under stress. In the same study, Whitesell & Lindquist (2005) describes the different functions a chaperone has in the cell. For example; chaperones help folding proteins, translocate proteins across membranes, do quality controls in the ER and control normal protein turnovers. Basically, chaperones can be described as "housekeeping" proteins. Whitesell & Lindquist (2005) gives the information that chaperones rarely work alone, often there are several other machineries in the cell that are involved when chaperones do their work. Proteins that the chaperones control are called "client proteins".

A great amount of client proteins of HSP90 have been shown to be signal transducers that are of great importance in growth control, developmental processes and cell survival (Whitesell & Lindquist, 2005). As the name implies, HSP90 helps stabilizing proteins during stressful environments, particularly heat stress. However, even under non stressful environments HSP90 still do some of its work. According to Whitesell & Lindquist (2005) the number of proteins that are thought to be interacting with HSP90 is very big and a great amount of these proteins have shown to be oncogenic which means the potential to cause cancer.

HSP90 has shown to be helping oncoproteins from misfolding and degradation, and cancer cells are highly dependent on HSP90 proteins (Trepel *et al.* 2010). Therefore HSP90 is a desirable target for cancer treatment. Trepel *et al.* (2010) suggests that by targeting HSP90, not only one oncogene is affected but several and this lead to the blocking of several pathways in cancer. Another important finding is that several of HSP90s' client proteins are proteins that are known for protection against radiation-induced cell death (Spiegelberg *et al.* 2015). Hence, targeting HSP90 with an inhibitor would be desirable for a better treatment where a lower dose of radiation can be used.

1.1.2 AT13387

As described above, HSP90 is a suitable target when treating cancer since it is involved in many oncogenic pathways (Murray *et al.* 2010). Though, by inhibiting HSP90 there are risks that toxicity levels would be too high in patients since HSP90 exist in all the cells. However, Murray *et al.* (2010) came to the conclusion that HSP90 is more active in cancer cells and therefore inhibition has been reasonably specific in cancer cells.

The most used target site for inhibition of HSP90 is the N terminal domain (Woodhead *et al.* 2010). This domain is part of the activation of HSP90. In this site hydrolysis of ATP occurs, since it is part of the activation of the chaperone, it makes a suitable target. Woodhead *et al.* (2010) describes that by using fragment screening and structure guided design researchers have come up with multiple suitable compounds that could inhibit HSP90 at this site. One of the compounds is AT13387. In the same study of Woodhead *et al.* (2010) it was shown that AT13387 has a strong affinity to the N terminal in HSP90. Due to this high affinity, the turnover of ATP to ADP cannot occur when AT13387 has bound to HSP90. Thus, HSP90 is no longer getting activated. AT13387 is made synthetically and is thereby fairly easy to synthetize in large-scale due to the synthetic tractability.

AT13387 is in clinical trials and has got the trade name Onalespib (Wagner *et al.* 2016). Since HSP90 has client proteins that protect cancer cells from dying of irradiation, the co-treatment of AT13387 and irradiation is examined due to the fact that AT13387 has been shown to possess radiosensitizing effects (Spiegelberg *et al.* 2015). Thanks to the radiosensitizing effects by AT13387 a lower dose of irradiation could technically be used in patients and is therefore a favourable drug to do further work with.

In contrast to other HSP90 inhibitors that have been in clinical trials, AT13387 does not show signs of hepatotoxicity in most of the patients (Shapiro *et al.* 2015). In the same study it was shown that in patients that showed signs of hepatotoxicity after treatment with AT13387 the effects were very mild. Hepatotoxicity is one of the greatest concerns when examining HSP90 inhibitors and has been the reason of the withdrawn of several drugs since it is damaging organs. Shapiro *et al.* (2015) showed that although AT13387 comes with side effects, such as diarrhea, nausea and vision disturbances such as a “blurry” vision and reduced night vision, the drug is tolerable in cancer patients and show effects on tumours and therefore should be further examined.

1.2 Aims and objectives

The aim of this master thesis was to examine and characterize AT13387 in combination with external beam gamma radiation in various human cell lines grown in monolayer cell culture. The goal has been to optimize drug administration and reveal mechanisms of AT13387 radiosensitization. To achieve this, multiple methods have been used, such as XTT assays, migration assays, flow cytometry and immunoblotting.

This project did not need to take in consideration any ethical aspects. No animal experiments have been performed, only *in vitro* studies have been used. The human cell lines that have been used during the project have been donated by patients who have given their consent for research to be made on the cells. The cell lines are anonymised but age, gender, prior treatment, cancer type and localization of the cancer is given.

1.3 Experimental procedures

In this project AT13387 was examined with and without irradiation. To be able to understand the mechanisms of AT13387 and what it does to the cells, different methods have been used during this work. Under this headline the methods are briefly described.

1.3.1 XTT assay

XTT assay is a type of colorimetric assay and can be used for investigating cell viability. The method is based on the metabolic activity within the cells and this activity is detected by using a microplate absorbance reader (Thermo fisher Scientific, 2017). This assay is dependent on a tetrazolium salt, XTT, mixed together with an electron-coupling reagent. With this mixture viable cells can convert the salt to a soluble formazan salt and since only viable cells can make this conversion the viability of the cells can be measured by reading the absorbance at your wanted wavelengths (Sigma-Aldrich, 2017).

1.3.2 Migration assay (wound healing assay)

An *in vitro* migration assay is as the name implies a method to study how cells migrate. The principle of this method is the creation of a scratch in a monolayer of cells and to follow up how long it takes for the cells to close the scratch. By taking pictures at the beginning when the scratch is made, and then repeat this at later time points, the distance and migration rate can be measured. This method has both advantages and disadvantages. It is a fairly simple method at low cost. It mimics to some extent migration of cells *in vivo.* However, this method requires a fairly large amount of cells and chemicals and compared to other methods it takes a longer time to perform the assay due to the fact that it takes time for the cells to form a monolayer and it takes time for the cells to close the scratch (Liang *et al.* 2007).

1.3.3 Flow cytometry

Flow cytometry is a method that can measure characteristics of single cells from cell populations. Each single cell can be measured by its different properties, such as size and internal complexity. Together with a sheath fluid each individual cell passes through an interrogation point in the flow cytometer. At this interrogation point a beam of monochromatic light hits the single cell. The emitted light from the cell is then spread in different directions and is collected via optics inside the instrument. The size is measured by forward light scatter and the internal complexity is measured by right angle scatter. In this method fluorescent dye is used for detection. By for example directly using fluorescently labelled antibodies a specific target in the cell can be detected. Or the use of unlabelled antibodies that bind a specific target in the cell, and then target the antibodies with a fluorescent molecule that later is detected in the flow cytometer (Brown & Wittwer, 2000).

1.3.4 Wide field microscopy

Wide field microscopy is a microscope technology that is based on using fluorescence to detect markers one is investigating in the cells. It has become an important tool in cell biology because one can easily detect what is inside a living specimen by using fluorescent molecular labels (Gustafsson, 2005). Wide field microscopy is constantly improving when it comes to the resolution. A resolution of 100 nm and below can be done today. Images of very complex biological specimens are possible and improving thanks to constant improvements with the resolution. The method is attractive because distribution and localization of wanted targets in the cells can be seen due to the emitted wavelengths from the fluorescent molecules (Stemmer *et al.* 2008).

1.3.5 Western blotting

Western blotting is a method used for the identification of a protein in a very complex mixture. By using an antibody to a specific target the method is very reliable. The method has two main steps for the separation of the wanted protein. First, the mixture is separated on a gel based on the size of the proteins. After this separation the proteins are transferred to a membrane, usually a nitrocellulose or a PVDF membrane by electrophoresis. It is on this membrane the primary antibody for the specific target can bind to the target. Later a labelled secondary antibody is added to target the primary antibody and the protein can now be detected, see figure 1 for a simplified explanation on how the method works. For the detection usually a CCD camera is used. It gives a large dynamic range and controls the exposure time easily.

What makes western blotting a preferable method when it comes to detecting and quantifying proteins are the highly sensitive-enhanced chemiluminescent substrates which makes the imaging of the targeted proteins clear and easy for analysis. The chemiluminescent substrates can detect proteins in very low concentrations. It is also possible to use fluorescence instead of chemiluminescent (Alegria-Schaffe *et al.* 2009).

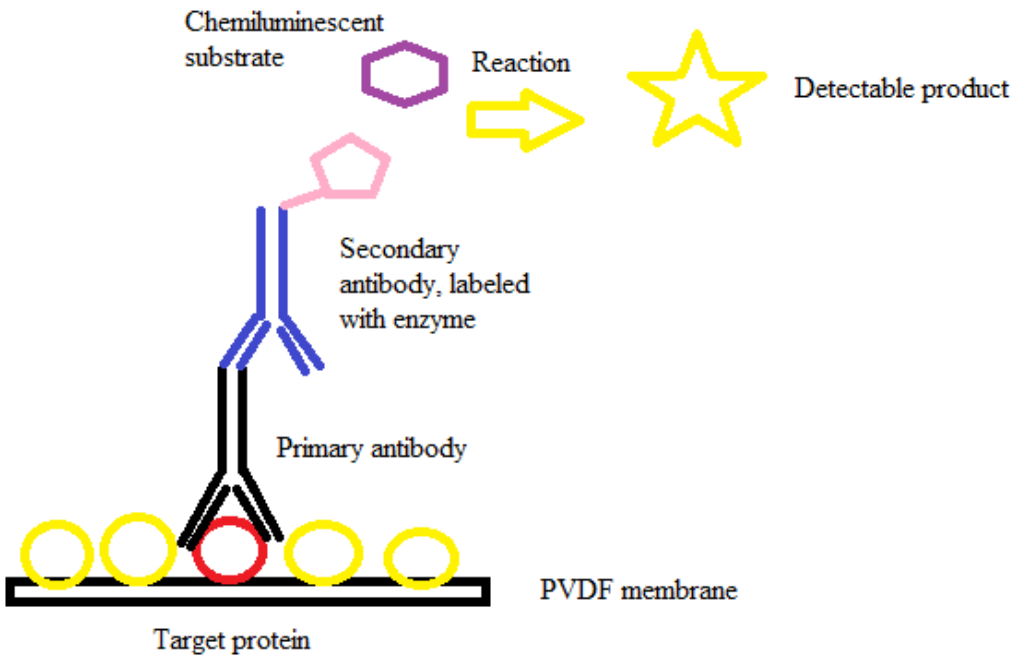

Figure 1: A modified figure from "Chapter 33 Performing and optimizing western blots with an emphasis on chemiluminescent detection" (Alegria-Schaffe *et al.* 2009) showing the idea of how western blotting works using a 2 step antibody staining.

2 Materials and methods

2.1 Cell lines

HCT116 (Horizon, UK): was cultured in RPMI 1640 complete medium (Biochrom GmbH, Germany) (500 ml RPMI 1640, 50 ml FCS, 5 ml Pest and 5 ml L-glut (Sigma Aldrich, Sweden)). HCT116 are colorectal carcinoma cells that derive from a male with colon ascendens and are a good model for colon cancer in humans (Ahmed *et al.* 2013). Cells were incubated at 37°C with 5% CO_2.

A431 (ATCC, USA): was cultured in HAM's F-10 complete medium (Biochrom GmbH, Germany) (500 ml Ham's F-10, 50 ml FCS, 5 ml Pest and 5 ml L-glut (Sigma Aldrich, Sweden)). A431 cells are squamous cell carcinoma cells that derive from human vulva. Squamous cell carcinomas are epithelial tumours and are common in head and neck cancer (Solomon e*t al.* 2003). Cells were incubated at 37°C with 5% CO_2.

GM5757 (NIGMS, USA): was cultured in MEM Earle's complete medium (Biochrom GmbH, Germany) (500 ml MEM Earle's, 50 ml FCS, 5 ml Pest and 5 ml L-glut and 5 ml vitamins (Sigma Aldrich, Sweden)). In this work, GM5757 cells were used as control cells. They derive from normal tissue. GM5757 cells are normal fibroblasts (Hartmann *et al.* 1995). Cells were incubated at 37°C with 5% CO_2.

2.2 Trypsinization

Cells that grow in monolayer can attach to each other and to the plastic surface in the bottle it grows in. Therefore, before cells are ready for usage in experiments, the cells need to be trypsinized so that they release from each other and the bottle. Trypsin is an enzyme that will cut the cells at specific connection sites.

Trypsin-EDTA (Biochrom GmbH, Germany) and complete sterile medium were warmed in a 37°C water bath. When the cell culture had grown enough and was ready for usage, old medium was removed. Approximately 1 ml trypsin-EDTA was added for a short wash before the trypsin-EDTA was removed with a vacuum suction. This step was repeated twice. Trypsin-EDTA was then added again (approximately 2-3 ml) and the bottle was put in the incubator, 37°C, 5% CO_2, for 5-15 minutes. After incubation, the cells should have released and were free in the trypsin-EDTA solution, approximately 10 ml complete medium was added, and the solution was resuspended 20 times. Cells were then ready for use.

2.3 Drug and radiation treatment

AT13387 (Selleckchem, USA) was first stored at -18°C as a powder. Before use, 10 mg was dissolved in 200 µl DMSO (Merck Millipore, Germany). AT13387 was diluted in complete sterile medium to achieve the desired concentrations. For XTT assays, cells were pre-plated and incubated with AT13387 (0.1, 0.3, 1, 3, 10, 30, 100 and 300 µM). 6 h after drug incubation some cells got irradiated using a ^{137}Cs ɣ-ray irradiator (Nordion Gammacell® 40 Exactor), at a dose-rate of 1.155 Gy/min for 6 min and 39 s. For the rest of the experiments used in this project cells were pre-plated and incubated with AT13387 (500 nM) and 6 h after drug treatment, wanted cells were irradiated with a ^{137}Cs ɣ-ray irradiator (Nordion Gammacell® 40 Exactor), at a dose-rate of 1.155 Gy/min for 6 min and 39 s, which exposed cells for a total of 6 Gy.

2.4 XTT assay

For this method cells were seeded in 96-well plates and three different time points were used for measurements (2, 4 and 6 h). For each cell line that was being investigated, two 96-well plates were seeded with cells. For HCT116 cells, 8000 cells/well were seeded and for A431 cells, 15 000 cells/well were seeded. On day 1, cells were seeded in the inner wells with 200 µl media and in the outer wells only complete medium was added. On day 2, if the cells were ~80% confluent in the wells, cells were treated with the different concentrations of AT13387 and 6 h later one of the two 96-well plates got irradiated.

On day 4 or 5, 7.5 ml of XTT reagent was mixed with 150 µl XTT activation reagent (ATCC, USA). The mixture was added to 15 ml complete medium. Old medium was removed from the plates and 150 µl of the new mix was added to each well containing cells. For a good comparison, the new mix was also added to 3 empty wells on each plate. Plates were

incubating at 37°C for two hours before the first measurements were taken. The instrument used for measurements was the BIO-RAD iMark^{TM} Microplate. The instrument measured at the wavelength 490 nm and 655 nm. Plates were then put back in the incubator and measurements were taken after 4 and 6 h. Figure 2 shows a simplified image on how the 96-well plates looked and which wells were treated.

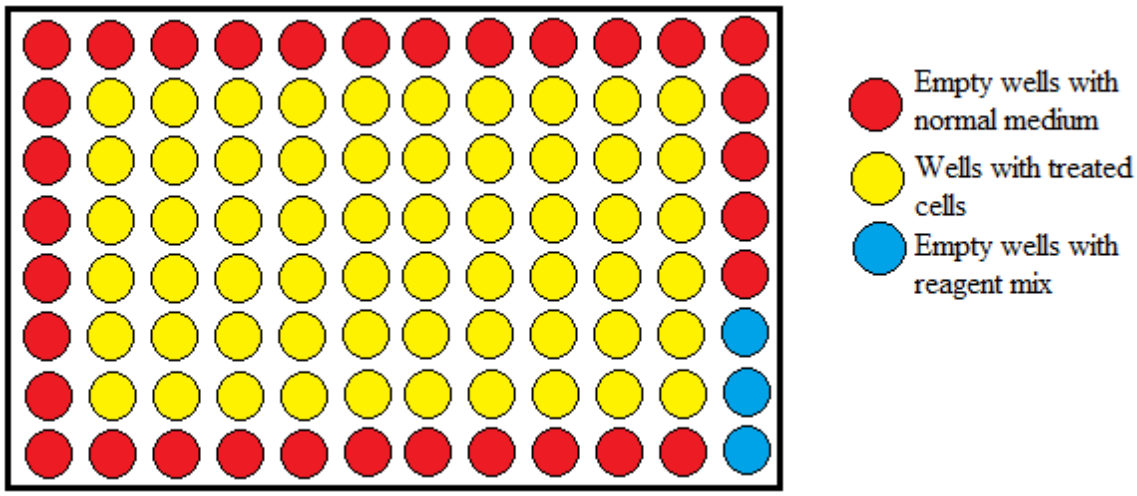

Figure 2: Simplified picture of the 96-well plates used in the XTT assays. The red wells demonstrate empty wells with media, the yellow wells demonstrate wells with seeded cells treated with different concentrations of AT13387 and blue wells demonstrate empty wells with only reagent mix.

2.5 Migration assay

For each cell line two 6-well plates were seeded with cells. An appropriate amount of cells were seeded such as on day 2 cells were about 80-90% confluent in the wells. In control and irradiation wells ~1 million cells were seeded and in AT13387 treated wells ~ 2 million cells were seeded. On day 2, a thin pipette tip was used to scratch a line in the middle of each well. One row in one of the plates was used as control and complete medium was added after old medium was removed. The other row was treated with medium containing 500 nM AT13387. The first row in the other plate was also treated with new complete medium and the other row with 500 nM AT13387, however 6 hours later this plate was irradiated. When medium was changed three areas were marked on the scratch with a pen and pictures were taken at those specific marks with a Canon EOS700D digital camera attached on an inverted Nikon Diaphot-TMD microscope. On day 3, 24 hours after cells were photographed the first time once again the marks were photographed. The scratch was analysed with help of ImageJ 1.51j and detection could be made on how far the cells had migrated towards each other. Figure 3 shows a simplified figure of the method.

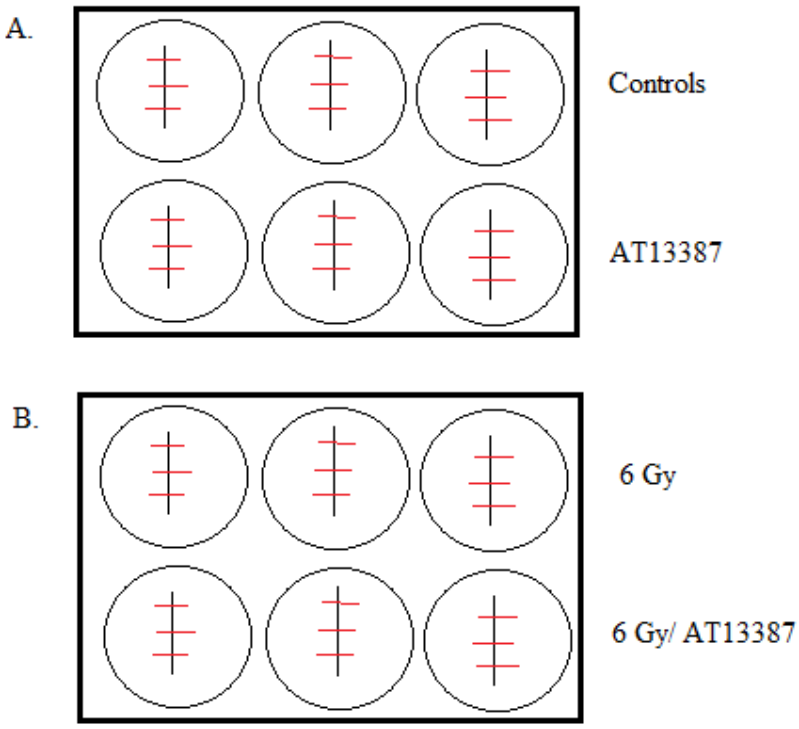

Figure 3: Simplified overview of a typical migration assay experimental setup. **A**) unirradiated control plate and **B**) irradiated plate. Cells were seeded in each well and treated with complete medium, AT1387, radiation and a combination of AT13387 and radiation. The black lines demonstrate the scratches and the red lines indicate the area were the pictures were taken. In total 9 pictures per treatment group were taken.

2.6 Flow cytometry

To investigate apoptotic cells and levels of HSP70 in the cells, cells were prepared for analysis with flow cytometry. For this method four different time points were used for measurements; 24, 48, 72 and 96 h. On day 1, cells were seeded in 16 culture flasks for each cell line, four flasks for each time point. The flasks were incubating at 37°C overnight with complete sterile cell culture medium. Within one time point the first flask was used as a control, the second flask was irradiated, the third was treated with AT13387 and the fourth flask was co-treated with AT13387 and irradiation.

On day 2, cells were treated with AT13387 and irradiation. In flask 3 and 4 medium with AT13387 was added, in flask 1 and 2 new complete medium was added. After 6 hours flask 2 and 4 was irradiated. Cells were then incubating at 37°C overnight. Except different treatments, cells were taken care of the same way all the time, which means if a flask was taken out from the incubator for irradiation the other flasks were also taken out from the incubator etc.

On day 3, cells for the first time point, 24 h, were fixated with ethanol. The cells were trypsinized (see *Trypsinization*) and transferred to falcon tubes. Tubes were centrifuged (Eppendorf Centrifuge 5810 R) at 1200 rpm for 5 min and medium was then removed. Pellets were dissolved with 0.3-0.4 mL ice-cold PBS. 1.2 mL 70% ice-cold ethanol was then gently added and cells were put in -18°C. On day 4, 5 and 6 cells for the other time points; 48 h, 72 h and 96 h were treated the same as the 24 h samples.

On day 7 (or later), cells were ready for analysis by flow cytometry. The fixed cells were centrifuged at 1200 rpm for 5 min at 4°C. Supernatants were removed without disturbing the pellets. The pellets were resuspended in 4 ml PERM buffer (1% BSA, 0, 1% Triton X-100). Once again cells were centrifuged at 1200 rpm for 5 min and supernatants were removed. ~400 000 cells were transferred to new falcon tubes and permeabilized in PERM buffer for 30 minutes. After that, cells were spun down, 1200 rpm for 5 min, and supernatants were removed. Cells were incubating over night with primary antibodies, either CASPASE-3, NOXA or HSP70 (abcam, UK), in PERM buffer at 4°C. 100 µl PERM buffer with CASPASE-3 [1:500] and NOXA [1:500] or HSP70 [1:100] was added to each tube, respectively.

The next day, 4 ml PERM buffer was added to each falcon tube. Tubes were centrifuged for 5 minutes at 1200 rpm. Supernatant was removed and secondary antibodies were added to target the primary antibodies. 100 µl PERM buffer was added together with secondary antibodies; anti-mouse FITC [1:400] and anti-rabbit APC [1:400] (abcam, UK) and tubes were incubating at room temperature for 30 minutes protected from light. After 30 minutes DAPI (1µg/ml, 10 µl/sample) was added to each sample and tubes were once again incubating at room temperature this time for 60 min. PERM buffer was added and cells were spun down at 1200 rpm for 5 min, and supernatants were removed. Cells were finally resuspended in 300 µl PERM buffer and transferred to FACS-tubes. The samples were analysed by using BD LSRFortessa™ (Biovis) with BD FACSDIVA™ Software and later data analysed with FCS express.

2.7 Wide field microscopy

40 000 cells for HCT116 cell line and 80 000 cells for A431 cell line and GM5757 cell line were seeded in chamber slides. Each cell line got four chambers, one used as control, one was irradiated, one was treated with AT13387 and the last one was treated with AT13387 and irradiation. Cells were put in incubator overnight, 37°C and 5% CO_2. The next day slides were washed in 1xPBS and fixated in ice-cold methanol overnight. 24 h after, washing in 1xPBS for 5 minutes and slides were blocked with 10% FBS (in 1xPBS) for 60 minutes in room temperature. Antibody solutions were prepared in 1% FBS (in 1xPBS), anti-53BP1 [1:1000] and Gamma H2AX [1:100] (abcam, UK) ~50 µl was dropped in each chamber. The slides incubated overnight in a moister chamber. The next day a solution with secondary antibodies was prepared in 1% FBS (in 1xPBS), Alexa 555 [1:400] and Alexa 488 [1:400] (abcam, UK). Slides were once again washed in 1xPBS, this time 3 times for 5 minutes.

Slides were incubated for 60 minutes at 37°C. The washing step was repeated. A DAPI (nuclear stain) solution was prepared (1 µg/ml) in ddH_2O and added to the slides, which were then incubated for 2 minutes in room temperature. Slides were washed 2 times for 5 minutes in 1xPBS. As a final step the slides were covered with Vecta Shield non hard set and sealed with nail polish. Slides were taken to the microscope (Zeiss AxioImager) and pictures were taken. Analysis was made with help of ImageJ 1.51n using custom macros.

2.8 Lysates for western blotting

In order to be able to analyse proteins in western blots, cell lysates have to be prepared that can be separated in electrophoresis.

Cells were seeded in flasks and grown in monolayer. Four time points were used, 24 h, 48 h, 72 h and 96 h for each cell line. Within every time point one flask was used as a control, and cells were grown in complete medium without anything added. One flask was exposed to irradiation, one flask was treated with AT13387 and the last flask was treated with AT13387 and exposed to irradiation.

When the time points had been reached cells were washed with 1-2 ml of cold PBS. Then 300-500 µl of lysis buffer (1% NP-40 alt, 20 mM Tris (pH 8.0), 137 mM NaCl, 10% glycerol, 2 mM EDTA, 1 mM heat activated sodium orthovanadate Na_3VO_4, (95°C for 10 min) and protease inhibitor cocktail (SIGMA)) was added to the flasks for about 30 minutes. The work was done on ice. After about 30 minutes the lysed cell-solution was transferred to Eppendorf tubes and centrifuged (MIKRO 200R, Hettish zentrifugen) for 15 minutes at 15 000 rpm in a cold centrifuge, 4°C. The supernatant was finally saved in marked Eppendorf tubes and stored at -18°C for later analysis with western blotting.

2.9 Western blotting

Earlier prepared lysates were thawed on ice. A solution of lysate, water and NuPAGE® LDS Sample buffer (4X) (Life technologies, USA) was added to Eppendorf tubes to a total of 20 µl. Concentration of proteins in lysates were measured with IMPLEN NanoPhotometer® P-class P360 and calculated before running western blot. The lysate with the lowest concentration determined how much of the rest of the lysates that were taken. 15 µl of the sample with the lowest concentration was mixed with 5 µl NuPAGE® LDS Sample buffer (4X). The samples were heated at 70°C for 10 minutes.

For this method either a Tris-Acetate 3-8% gel or a Bis-Tris 4-12% gel (Thermo Fisher Scientific, USA) was used, the gel was put in an electrophoresis chamber and the chamber was filled with 1 x TA running buffer (Tris-Acetate gel) or MOPS buffer (Bis-Tris gel), respectively. Each well on the gel was loaded with 10 µl of the mixed solutions and two ladders. Thermo Scientific PageRuler Prestained Protein Ladder (Thermo Fisher Scientific, Lithuania), as used on each side of the gel, 4 µl. The samples were always loaded in the same

order, starting with 24 h samples; control, 6 Gy, AT13387 and 6 Gy/AT13387. After the 24 h samples, 72 h and 96 h samples were following in the same order. After loading the gel, the gel ran at 150 - 200 V for ~1 h (BIO-RAD, POWER PAC 300). When markers on the gel nearly reached the bottom the gel was transferred to a PVDF-membrane (Merck Millipore, Germany) in transfer buffer with 20% MeOH (Merck Millipore, Germany) at 4°C. This time the gel ran at 100 V for 2 h. After 2 h the membranes were blocked with 5% BSA, PBS, 1% Tween for 1 h and cut in smaller pieces. The different pieces were incubated with primary antibodies at 4°C overnight on a rocking table. Primary antibodies used: Gamma H2AX [1:2000], ß-ACTIN [1:10 000], HSP90 [1:30 000], HSP70 [1: 1000], EGFR [1:5000] and VEGFR [1:2500] (abcam, UK). Antibodies were diluted in 5% BSA, PBS, 1% Tween.

The next day membranes were washed in PBS-T 3 times for 5 minutes on a rocking table. After washing, membranes incubated with secondary antibodies for 1 hour in room temperature on a rocking table. Secondary antibodies used, anti-rabbit, [1:30 000] and anti-mouse, [1:10 000] (Thermo Fisher Scientific, Sweden) were diluted in 1% BSA PBS-T. Membranes were once again washed with PBS-T 3 times for 5 minutes on a rocking table. Finally a substrate solution was mixed, Immobillon (Millipore, USA) 1:1 and each membrane incubated in the solution for 1 minute before scanning and taking picture of the membrane (FUJIFILM, Intelligent Dark Box II).

2.10 Statistical analysis

The data received from the experiments have been processed in Microsoft office Excel 2010 and all graphs have been plotted in GraphPad Prism 7. Statistical analyses have been performed on results from the XTT assays and migration assays using unpaired t tests in GraphPad Prism 7.

3 Results

3.1 XTT assay

Viability assays were performed to analyse the cells viability after treatments with different concentrations of AT13387 alone, compared to cells treated with the same concentrations of AT13387 but also irradiated with gamma rays. Cells were treated with the different treatments and 24 h after, measurements were taken. As shown in figure 4 the viability for cells in both cell line A431 and HCT116 goes down to almost 0 % after treatments. However, there are barely any differences between cells that are treated with AT13387 alone or cells from the combination treatment of AT13387 together with irradiation. Though, it is important to remember that the red and blue curves in figure 4 are normalized separately. Experiments have been repeated at least 3 times and the results are pooled together.

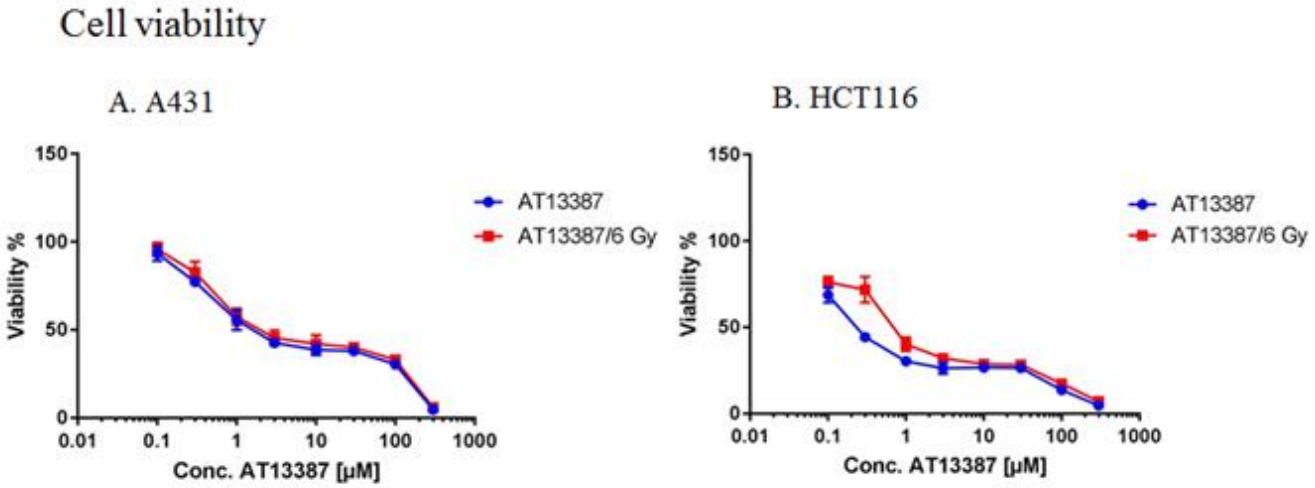

Figure 4: A. Pooled data of experiments for the viability of cells from cell line A431 after different treatments of AT13387 and the combination of AT13387 and radiation. Blue curve is showing cells treated with different concentrations of AT13387 alone. Red curve is showing cells treated with the combination treatment of different concentrations of AT13387 together with irradiation (n=3, error bars = SD). **B**. Demonstrates the same thing as figure A, but for cell line HCT116 (n=2, error bars = SD).

3.2 Migration assay

Migration assays were performed to analyse the migration capacity of the cells after different treatments. The migration capacity is reduced after treatment with AT13387 alone and with a combination treatment of AT13387 and radiation for both cell lines A431 and HCT116. Figure 5 shows representative images of the migration assays after no treatment and treatment with AT13387 and irradiation, respectively. Even though the error bars are quite big and there is no big difference between AT13387 alone compared to AT13387 and irradiation, these results show a trend that treatment with AT13387 and AT13387 combined with irradiation is affecting the migration capacity of the cells much more than just irradiation, see figure 6. In this experiment GM5757 cells were also tested and it is clear that non cancer cells are also affected after treatment with AT13387, however this is not surprising since the inhibitor will also inhibit HSP90 to some extent in normal cells.

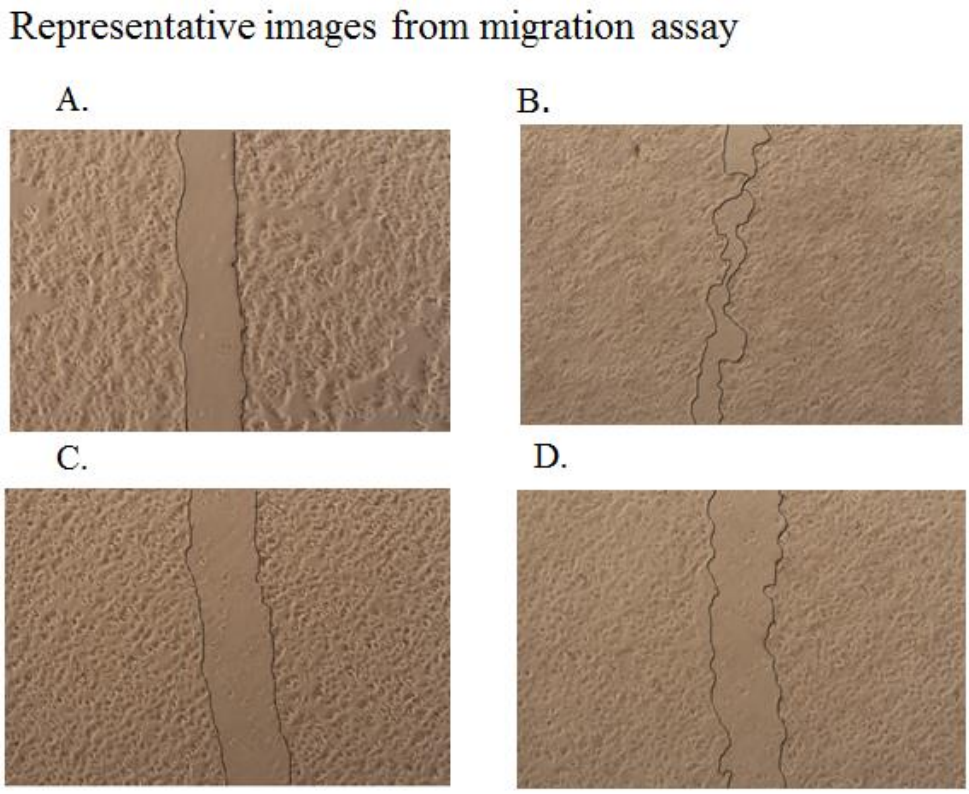

Figure 5: Representative images of the migration analysis at time point 0 and at 24 h. **A**. Show cells after a scratch has been made at time 0. **B**. Shows the same scratch as in A, but at time point 24 h, no treatments have been given the cells. **C**. Cells after a scratch have been made at time 0. **D**. The same scratch as in C but at time point 24 h, here cells have been treated with AT13387 and radiation.

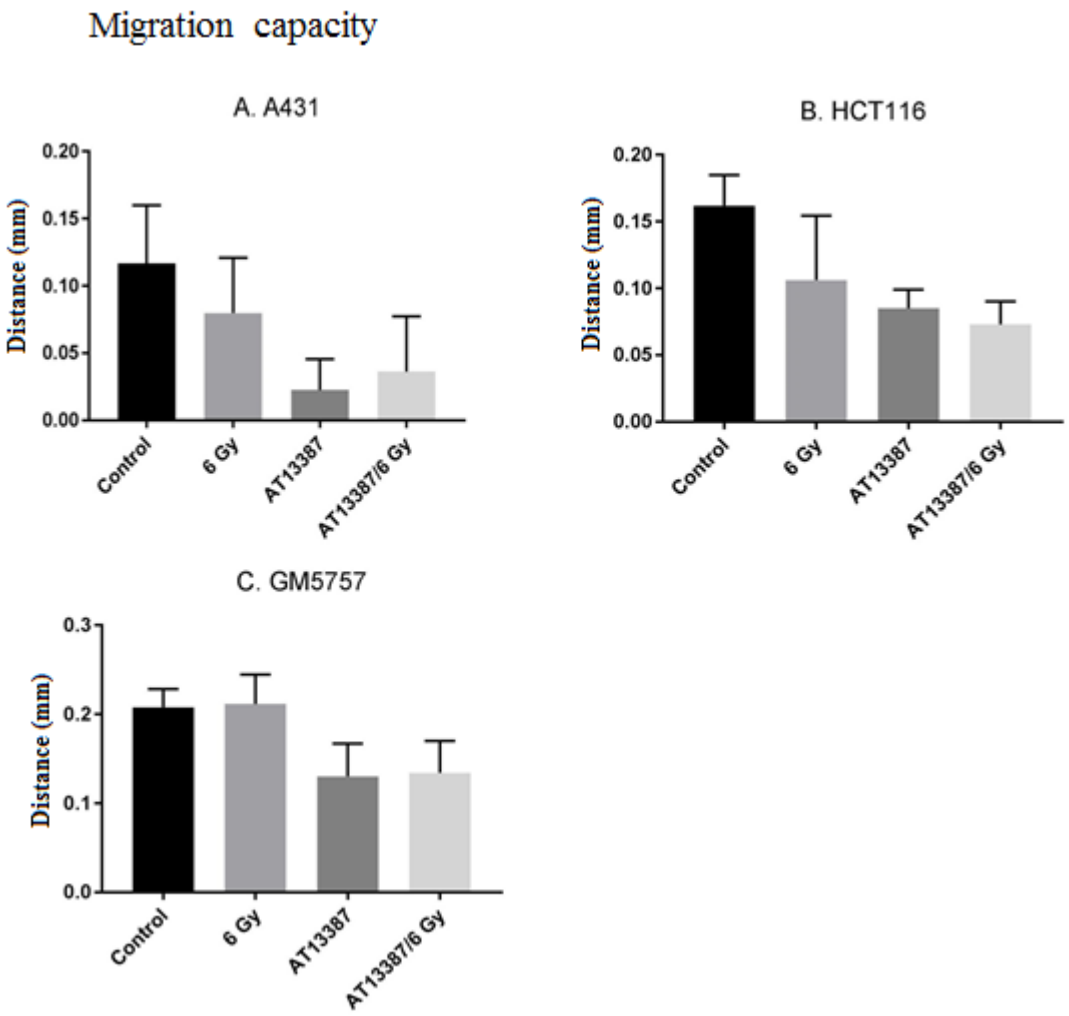

Figure 6: A. Shows how the migration capacity varies after different treatments of radiation, AT13387 and AT13387/radiation on cell line A431. **B**. Demonstrate migration capacity for cell line HCT116 after different treatments of radiation, AT13387 and AT13387/radiation. **C**. Shows how the cell line GM5757 has migrated after different treatments of radiation, AT13387 and AT13387/radiation. The distance the cells have migrated, for all cell line, has been calculated as ((distance at 0 h)-(distance at 24 h))/2, (n=1, error bars= SD).

3.3 Flow cytometry

3.3.1 HCT116 cells

Figure 7 demonstrates results of expression of HSP70 in HCT116 cells after different treatments of radiation, AT13387 and AT13387/radiation. The levels of HSP70 are examined due to the fact that HSP70 is taking over HSP90's function when HSP90 is inhibited. In the earliest and latest time points an up regulation of HSP70 can be seen with the combination treatment of AT13387 and radiation. The levels of HSP70 during the other measurements stay relatively stable, see figure 8. HSP70 is also a heat shock protein with similar function as HSP90. This result supports already published data which is showing this trend of an increase of HSP70 when HSP90 is inhibited (Chiosis *et al.* 2004).

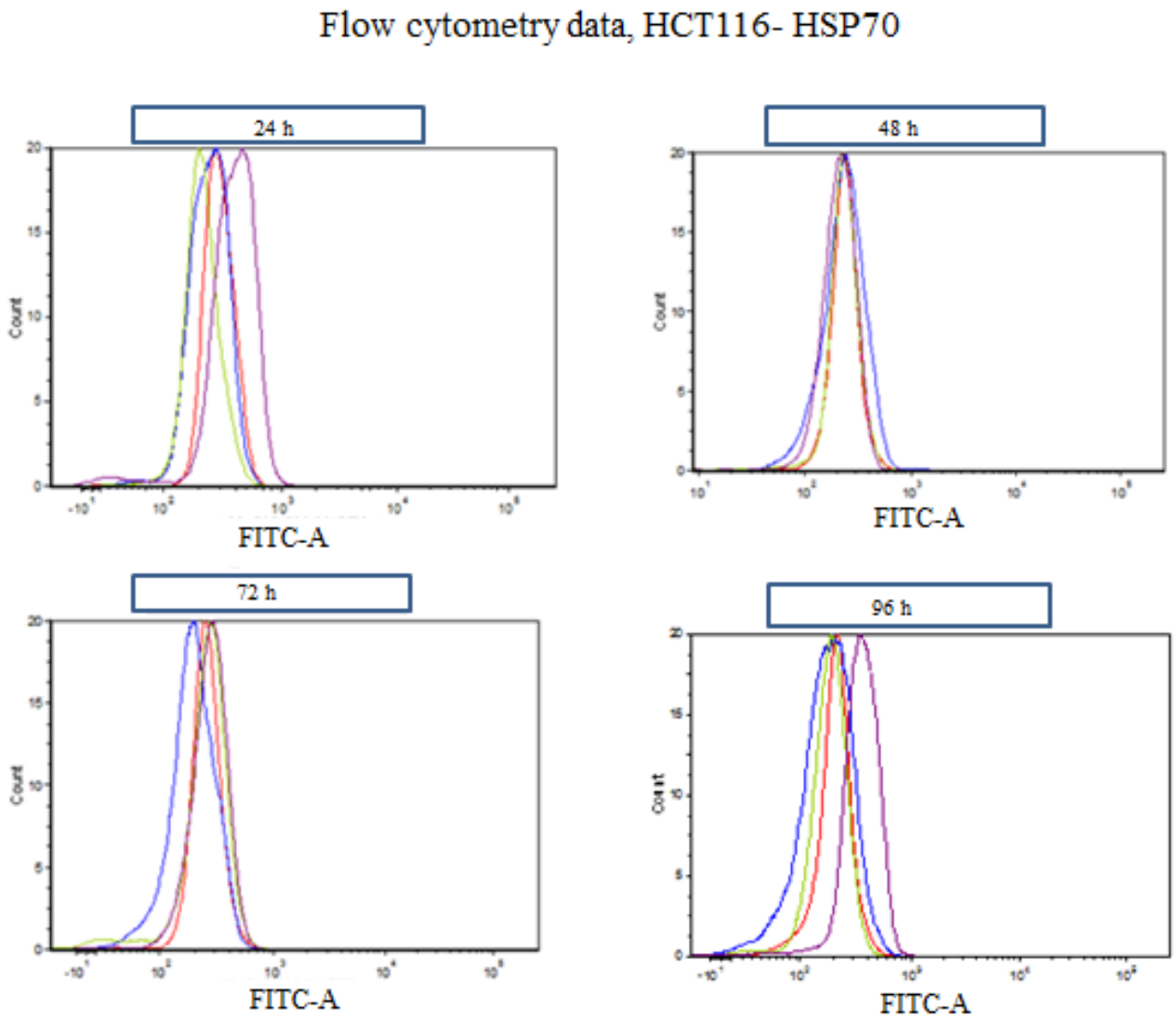

Figure 7: Images are demonstrating the variation of HSP70 levels in HCT116 cells at four different time points and treatments with radiation, AT13387 and AT13387/radiation. Red curve is showing the control cells, blue curve is cells that have been irradiated, green curve represent cells that have been treated with AT13387 alone and purple represent cells of the combination treatment with AT13387 and irradiation. The top left square are results after 24 h following squares are results after 48 h, 72 h and 96 h, respectively (n=1).

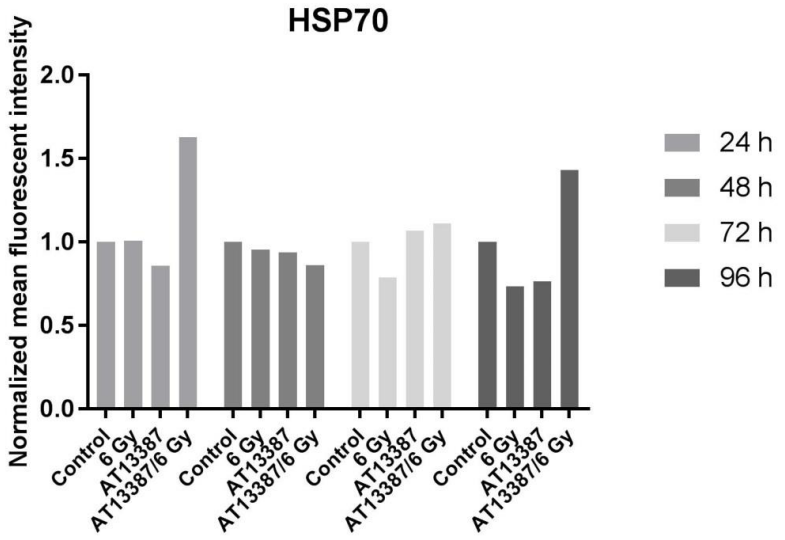

Figure 8: Demonstrates the expression levels of HSP70 after different treatments on cell line HCT116. It is calculated from the curves in figure 7, where the mean fluorescent intensity value of the different treatments is divided by the mean fluorescent intensity value for the controls. The biggest difference is seen with the combination treatment AT13387 and irradiation at the 24 and 96 h time point, respectively, where HSP70 is highly up regulated (n=1).

The levels of CASPASE-3 in HCT116 cells were also investigated. CASPASE-3 is a death protease that mediates apoptosis (Porter & Jänicke, 1999). It was therefore of interest to investigate if HSP90 inhibition and irradiation would cause an increased expression level of CASPASE-3. If this would be the case, it would indicate that cells after treatment start to be more apoptotic. As shown in figure 9 there is an increase of CASPASE-3 for the combination treatment after 24 h and after 96 h. However, in the time points in between the difference is not as big, see figure 10.

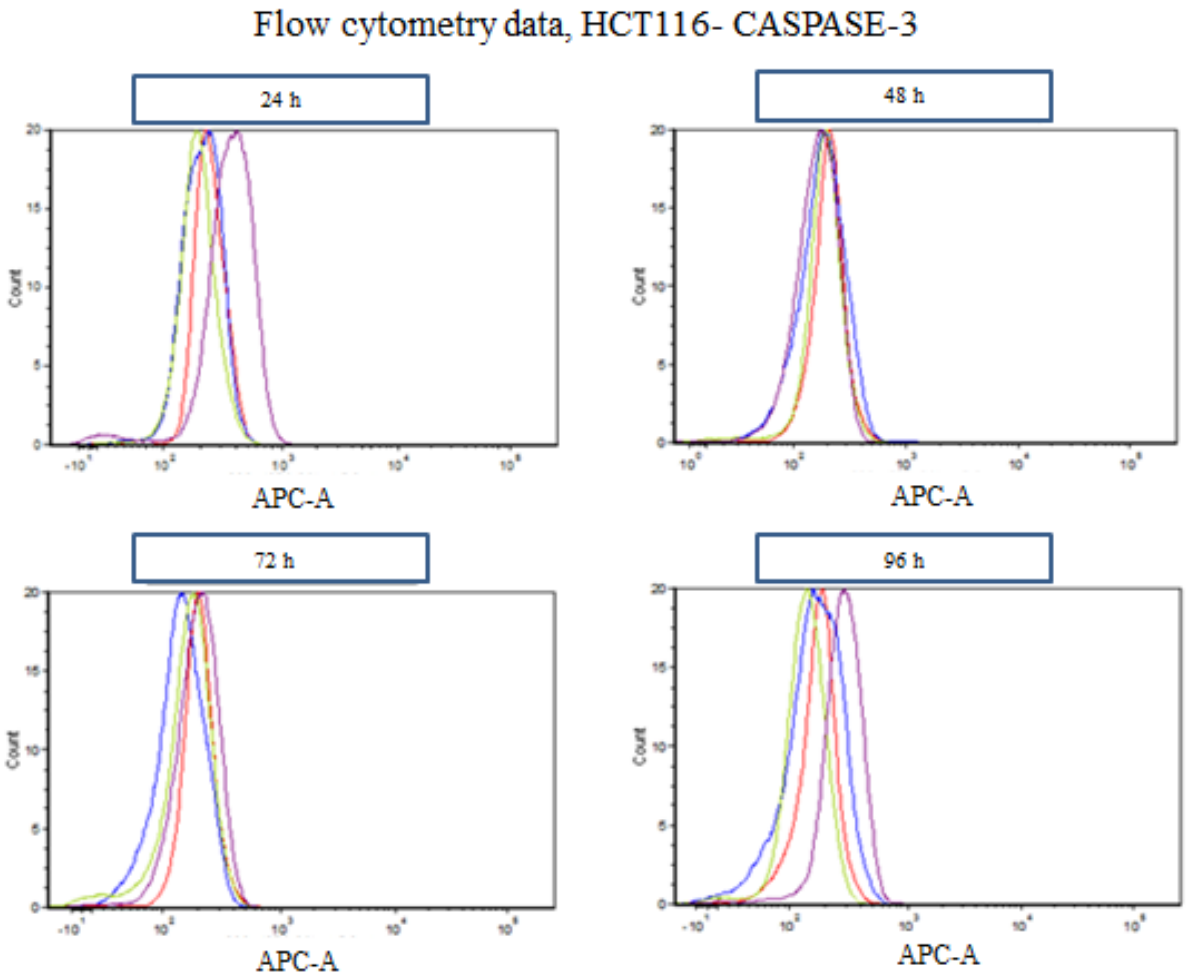

Figure 9: Images are demonstrating the variation of CASPASE-3 levels in HCT116 cells at four different time points and treatments with radiation, AT13387 and AT13387/radiation. Red curve is the control cells, blue is cells that have been irradiated, green curve represent cells that have been treated with AT13387 alone and purple represent cells of the combination treatment with AT13387 and irradiation. The top left square are results after 24 h following squares are results after 48 h, 72 h and 96 h, respectively (n=1).

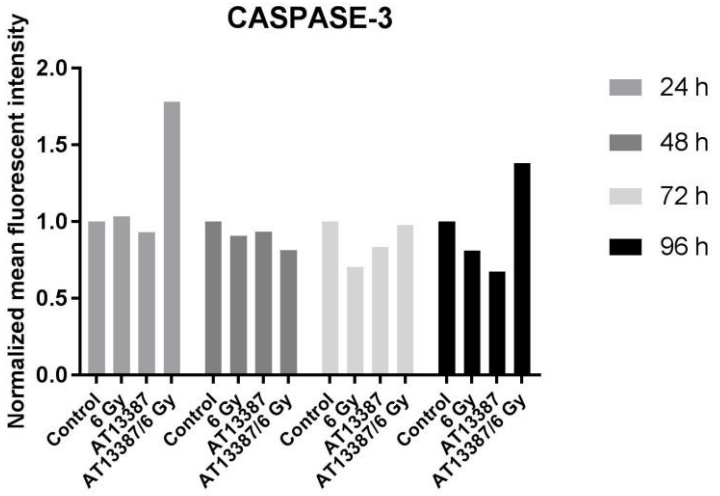

Figure 10: Demonstrates the expression levels of CASPASE-3 after different treatments on cell line HCT116. It is calculated from the curves in figure 9, where the mean fluorescent intensity value of the different treatments is divided by the mean fluorescent intensity value for the controls. The biggest difference is seen with the combination treatment AT13387 and irradiation at the 24 and 96 h time point, respectively, where CASPASE-3 is highly up regulated (n=1).

3.3.2 A431 cells

The levels of expression of NOXA protein were also examined. NOXA is a protein that has shown to be involved in apoptosis of cells (Sun & Leaman, 2005). It is a mitochondrial protein that disrupts the outer membrane of the mitochondria. This process is contributing to apoptosis. As shown in figure 11 and 12 there is no increase in NOXA levels for cells that have been treated with AT13387 alone or the combination treatment AT13387/irradiation. For each time point the NOXA levels stay relatively the same. From these result it does not look like cells are getting more apoptotic from the treatments.

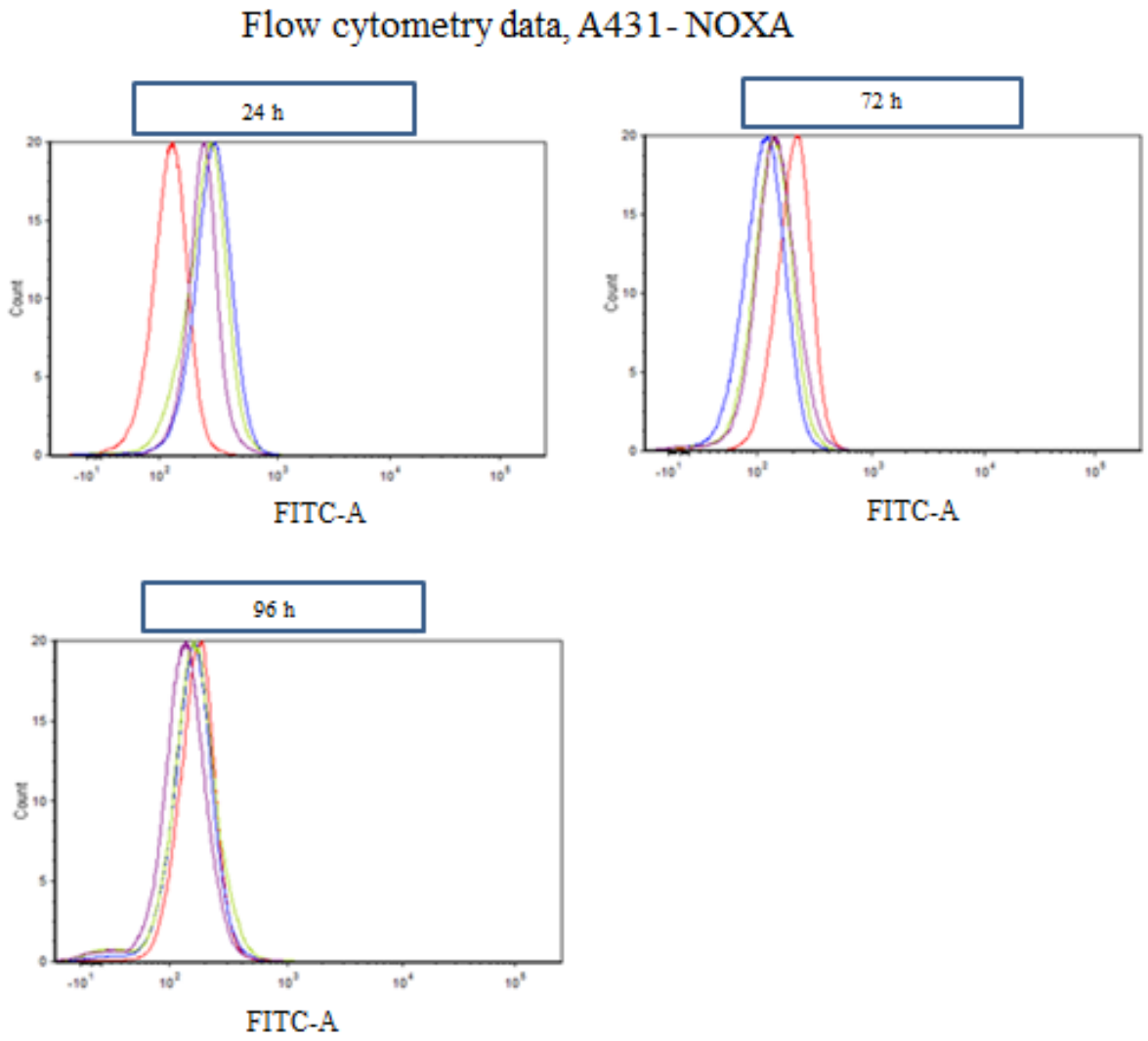

Figure 11: Images are showing the variation of NOXA in cell line A431 after treatment with radiation, AT13387 and AT13387/radiation. Red curve is the control cells, blue curve is cells that have been irradiated, green curve represent cells that have been treated with AT13387 alone and purple represent cells of the combination treatment with AT13387 and irradiation. The top left square are results after 24 h following squares are results after 72 h and 96 h, respectively (n=1).

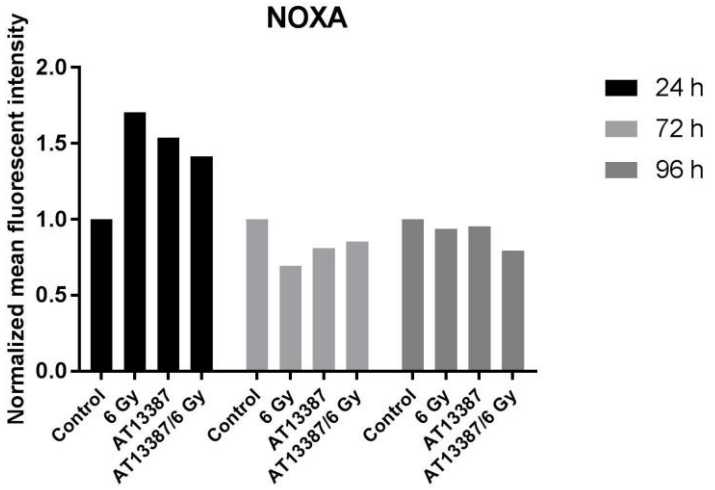

Figure 12: Represents the variation of expression levels of NOXA after the different treatments, radiation, AT13387 and AT13387/radiation, on cell line A431. It is calculated from the curves in figure 11, where the mean fluorescent intensity value from the different treatments is divided by the mean fluorescent intensity value for the controls. The NOXA protein does not vary much within each time point (n=1).

The levels of CASPASE-3 were also examined in A431 cells. For later time points there are some indication of higher levels of CASPASE-3 in cells treated with AT13387 alone and AT13387/irradiation, however there are no direct difference between them. From these results it looks like treated cells for later time points are a bit more apoptotic than cells that just have been irradiated, see figure 13 and 14.

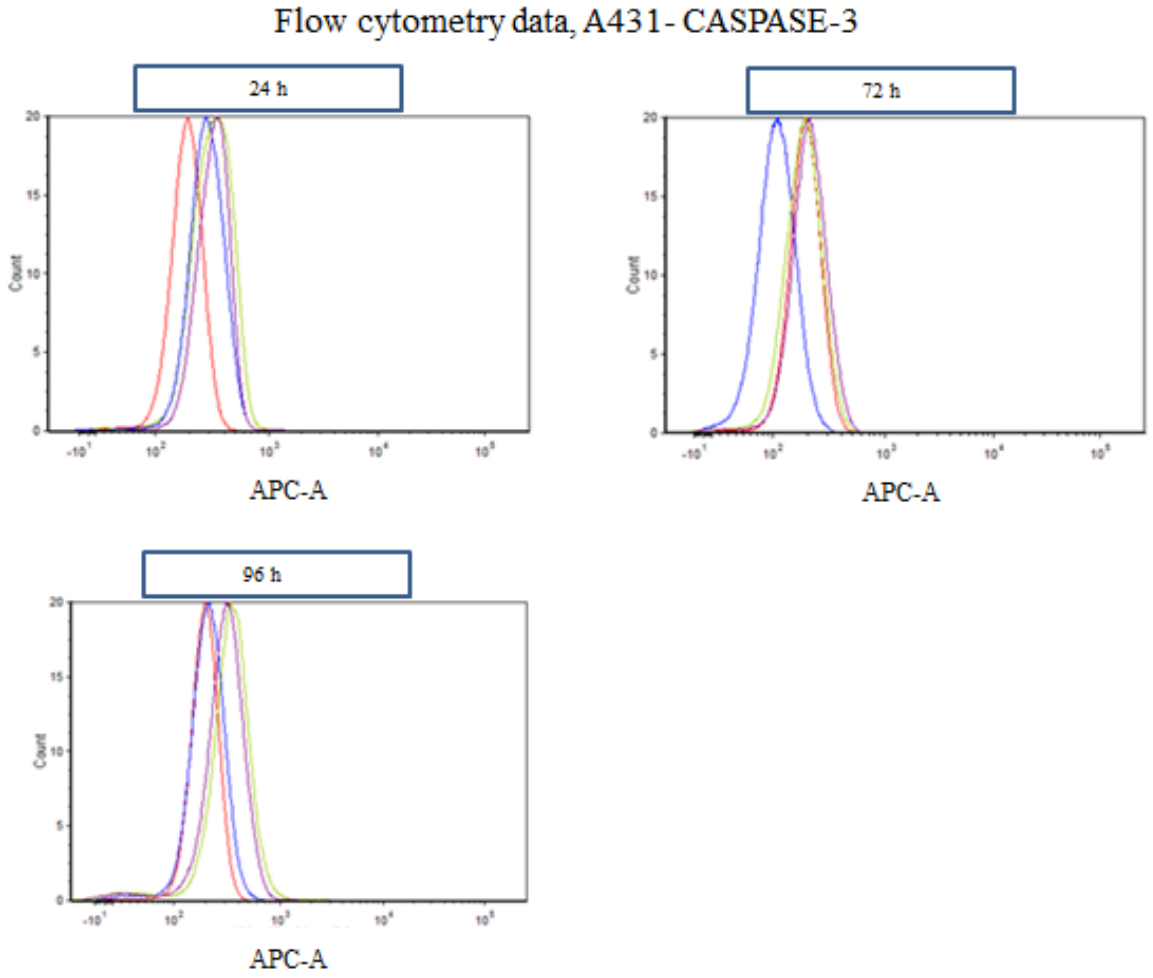

Figure 13: Images are demonstrating the variation of CASPASE-3 in A431 cells after treatment with radiation, AT13387 and AT13387/radiation. Red curve is showing the control cells, blue is cells that have been irradiated, green curve represent cells that have been treated with AT13387 alone and purple represent cells of the combination treatment with AT13387 and irradiation. The top left square are results after 24 h following squares are results after 72 h and 96 h, respectively (n=1).

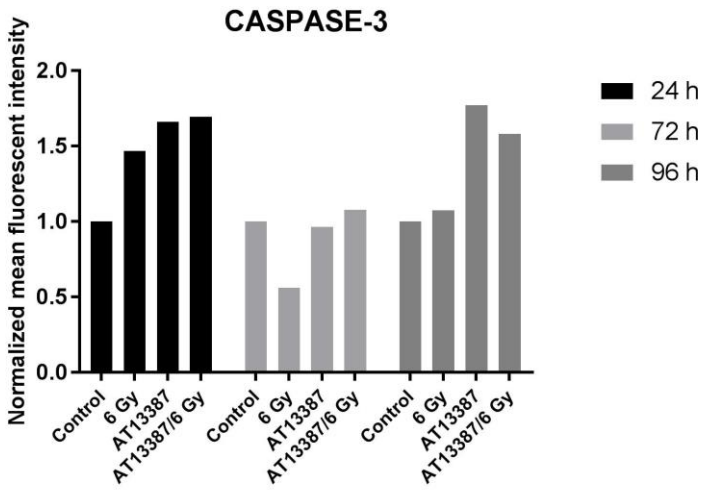

Figure 14: Expression levels of CASPASE-3 after different treatments on cell line A431. It is calculated from the curves in figure 13, where the mean fluorescent intensity value from the different treatments is divided by the mean fluorescent intensity value for the controls. The biggest difference is seen in the later time point, 96 h, for both treatment with AT13387 alone and the combination treatment AT13387 and irradiation (n=1).

3.4 Wide field microscopy

Wide field microscopy was performed to investigate the amount of DNA double strand breaks in the nucleus of the cells. Double strand breaks can trigger both growth stop and cell death. 53BP1 is a protein that is of importance when it comes to repairing the double strand breaks in the nucleus. The protein binds to the damaged DNA and recruits other important proteins for the repair (Panier & Boulton, 2013). Therefore targeting 53BP1 gives the information on how many double strand breaks there are in the cell. Figure 15 is showing representative images from the assay where different treatments have been given the cell lines, these particular images are GM5757 cells. The red colour is showing the nucleuses in the cells and the small grey dots are representing 53BP1. Figure 16 demonstrates how the double strand breaks vary for A431 cells, HCT116 cells and GM5757 cells after different treatments. From these results the combination treatment AT13387 and irradiation gives the highest number of double strand breaks for all the cell lines.

Representative images from wide field microscopy

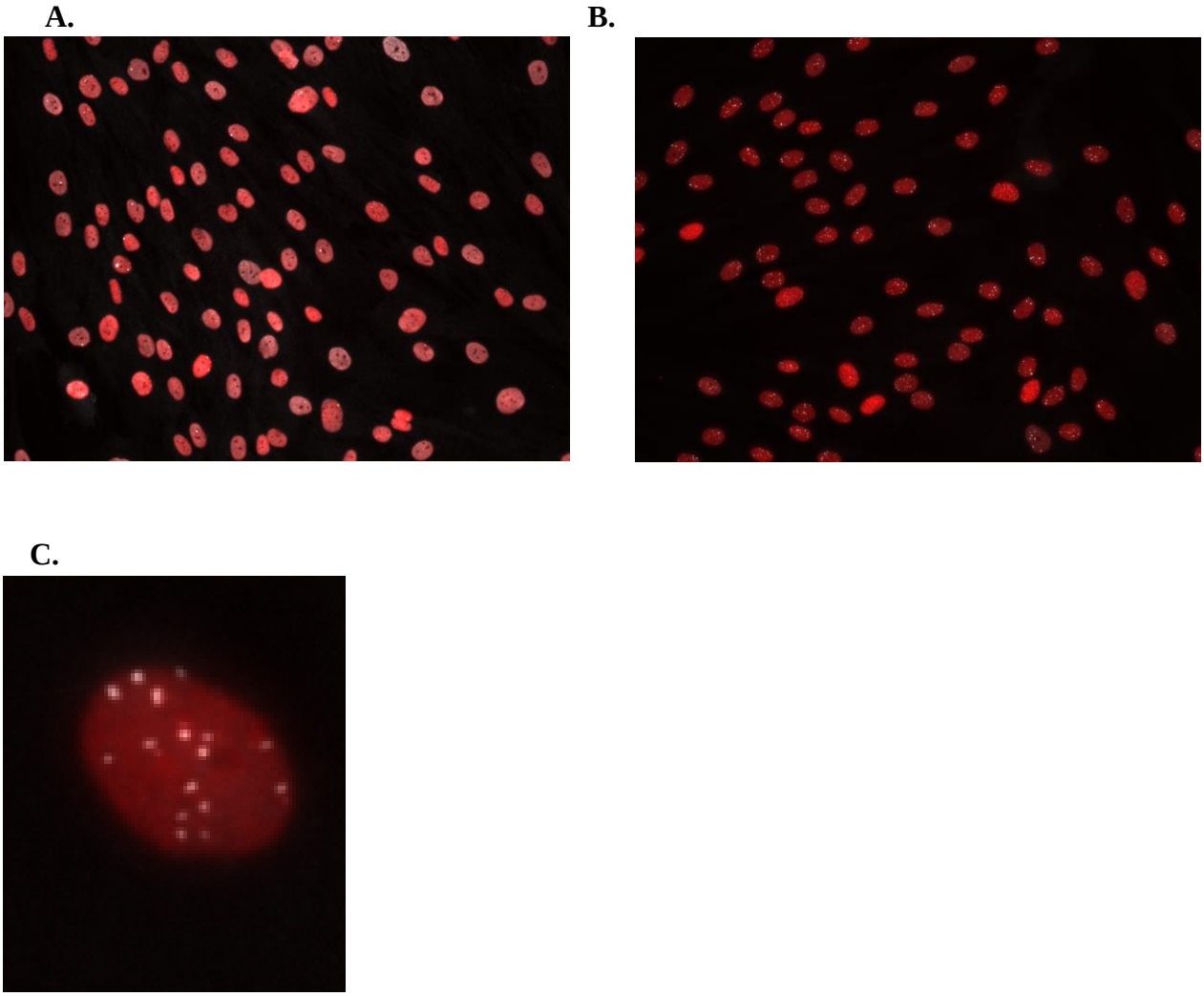

Figure 15: A. Representative image of GM5757 cells after no treatment. **B**. Representative image of GM5757 cells after treatment with AT13387 and radiation. The red colour is demonstrating the nucleuses in the cells and the grey dots are 53BP1 proteins, indicating DNA damage. **C**. Image of one enlarged cell after treatment with AT13387/radiation as in B. All the pictures are taken 24 h after treatments.

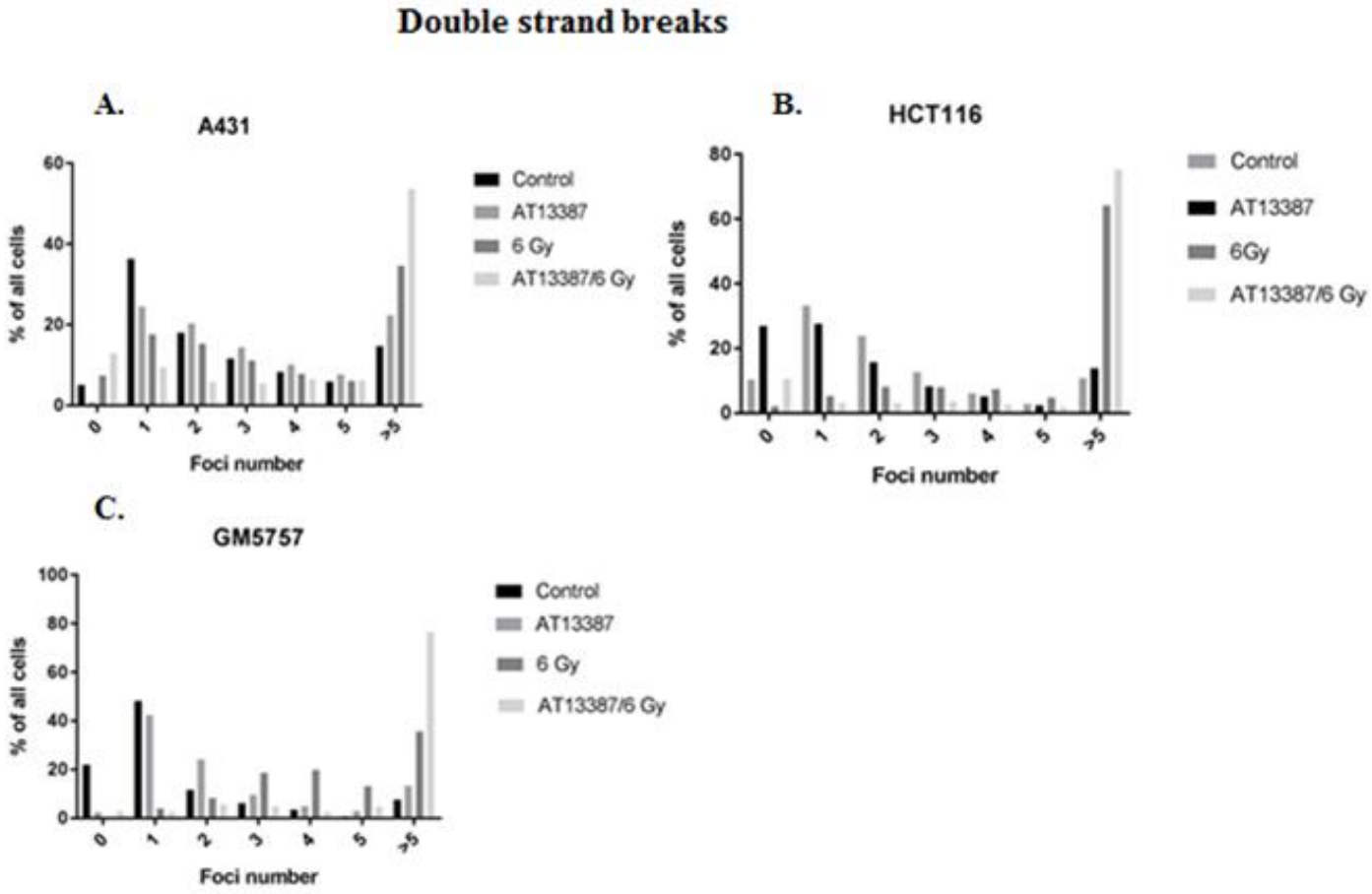

Figure 16: Demonstrate how the different treatments, radiation, AT13387 and AT13387/radiation, affect DNA damage in the **A.** A431 cells, **B**. HCT116 cells and **C**. GM5757 cells. In all cell lines biggest numbers of double strand breaks are seen with the combination treatment (n=1).

3.5 Western blotting

3.5.1 A431 cells

Several interesting proteins have been investigated with western blotting in order to understand the mechanisms behind the treatment with AT13387 and AT13387 and irradiation, respectively. In this experiment, ß-ACTIN has been used as a control protein so that the same amount of each sample is loaded on the gel. ß-ACTIN can be used as a control since it is not known that it is involved in any of HSP90s pathways. From these results for A431 cells, we can happily draw the conclusion that VEGFR, which is a receptor for the endothelial growth factor VEGF and is known to play a role in cancer due to its involvement in pathological angiogenesis (Shibuya, 2011), is down regulated in the later time points after treatment with AT13387 and AT13387 and irradiation, respectively, see figure 17 and 18. Interestingly HSP90 seems to be up regulated in the later time points after inhibition of it, see figure 17 and 18. The idea behind testing what is happening with HSP70 after inhibition of HSP90 is that in theory it would be up regulated and "take over" HSP90s functions since they are so similar. Interestingly the idea seems to be right, HSP70 is up regulated see figure 17 and 18. Another interesting protein that has been investigated is ɣH2AX. By looking at the expression levels

of ɣH2AX it can tell us if the cells have a lot of DNA damage. ɣH2AX is the first protein that is involved in recruitment and localization of DNA repair proteins (Kuo & Yang, 2008). Surprisingly, in A431 cells, ɣH2AX is highly expressed only in the first time point after treatment with AT13387 and AT13387 and irradiation, see figure 17 and 18. There are no signs of high expression of ɣH2AX in the later time points after treatment, which indicates that the cells have managed to recover in the later time points but not after 24 h. EGFR has also been tested. EGFR is a known client protein of HSP90 and is known for its role in cell survival after treatment with chemotherapy and radiotherapy (Ahsan *et al.* 2012). Here we show a clear down regulation of EGFR in the later time points, see figure 17 and 18. This supports previously published data (Spiegelberg *et al.* 2015) and is what was expected after treatment with AT13387 and AT13387 and irradiation, respectively.

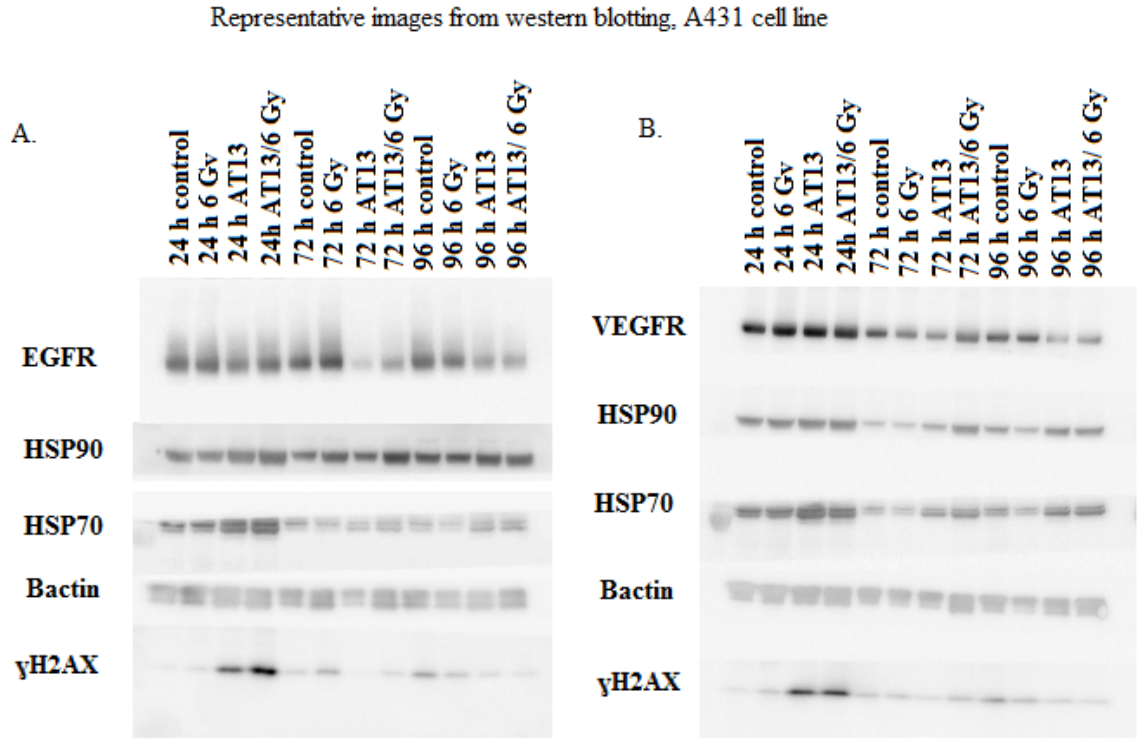

Figure 17: A. Representative image of the results from western blotting for the A431 cell line. Here ß-ACTIN is used as a control protein. Proteins investigated in this assay were EGFR, HSP90, HSP70 and ɣH2AX. **B**. One more representative image of the results from western blotting for the A431 cells. The difference from A is that here also the expression of VEGFR is investigated.

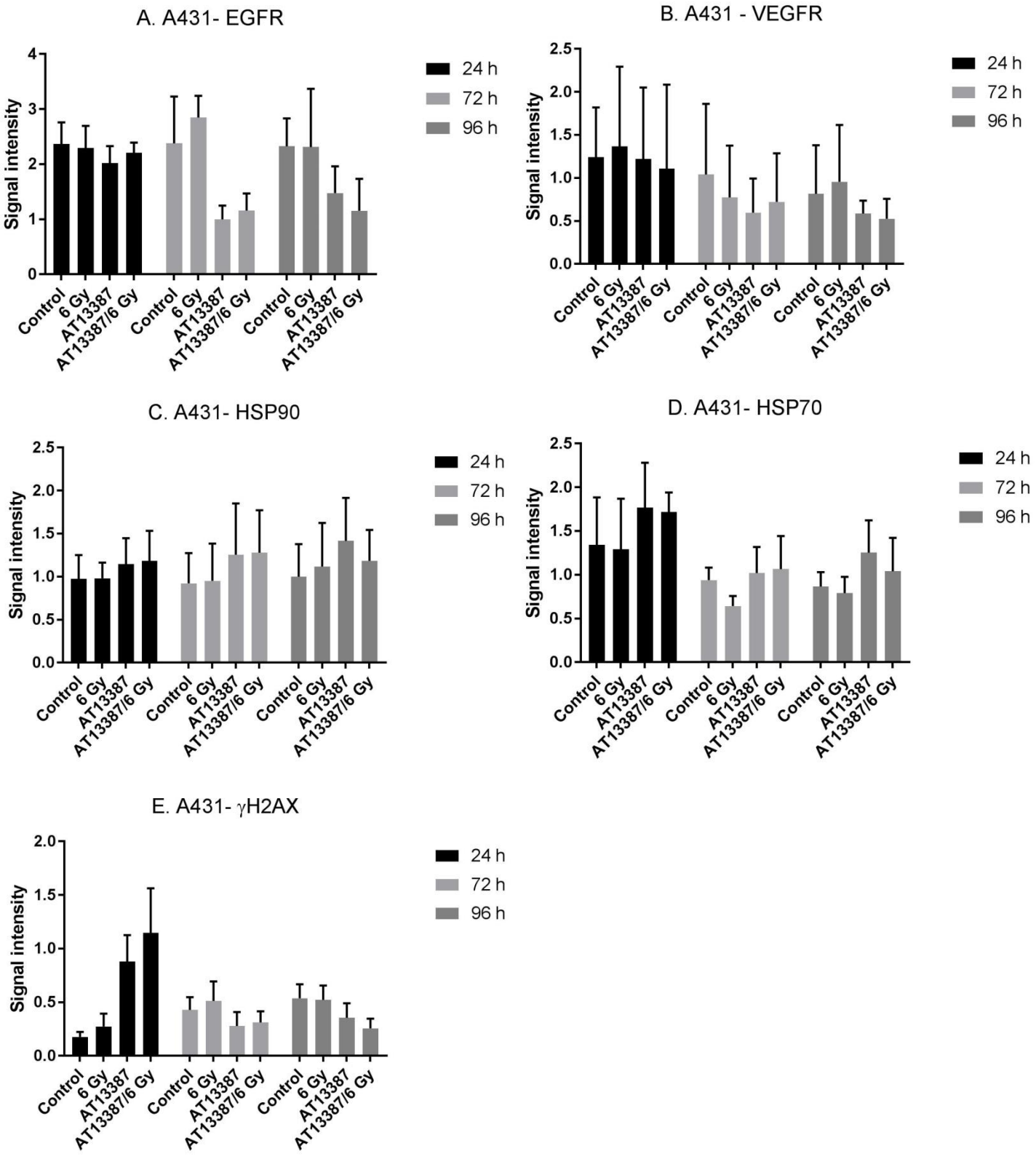

Figure 18: All the figures represent graphs translated from figure 17 with the use of ImageJ. **A**. Is showing how EGFR varies through the different treatments and after different time points. In the later time points, 72 h and 96 h EGFR is down regulated after treatments with AT13387 and AT13387 and irradiation, respectively (n=3, error bars= SD). **B**. Show results from western blotting for VEGFR, in the latest time point treatments with AT13387, and AT13387 and irradiation is clearly down regulated (n=3, error bars = SD). **C**. Represents results from western blotting when looking at HSP90. In all time

points HSP90 is slightly up regulated after treatments with AT13387 with or without irradiation (n=6, error bars = SD). **D**. Is showing results for HSP70 after western blotting, in all time points HSP70 is slightly up regulated after treatments with AT13387 alone and AT13387 combined with irradiation (n=5, error bars = SD). **E**. Demonstrates how ɣH2AX varies throughout the different treatments and time points. In the first time point ɣH2AX is highly up regulated after treatments with AT13387 with and without irradiation (n=6, error bars = SD).

3.5.2 HCT116 cells

Same proteins as for A431 cells have been investigated for HCT116 cells. The results follow the same trends as for the A431 cells except for VEGFR, where the down regulation does not seem to happen as it does for the A431 cells. It also seems like DNA damage is worse in later time points in HCT116 cells compared to A431 cells since ɣH2AX is up regulated in all time points after treatment with AT13387 alone and the combination treatment AT13387 and irradiation. The other proteins, HSP90 and HSP70 show trends of up regulation same as for A431 cells. The client protein EGFR is distinctly down regulated, see figure 19 and 20.

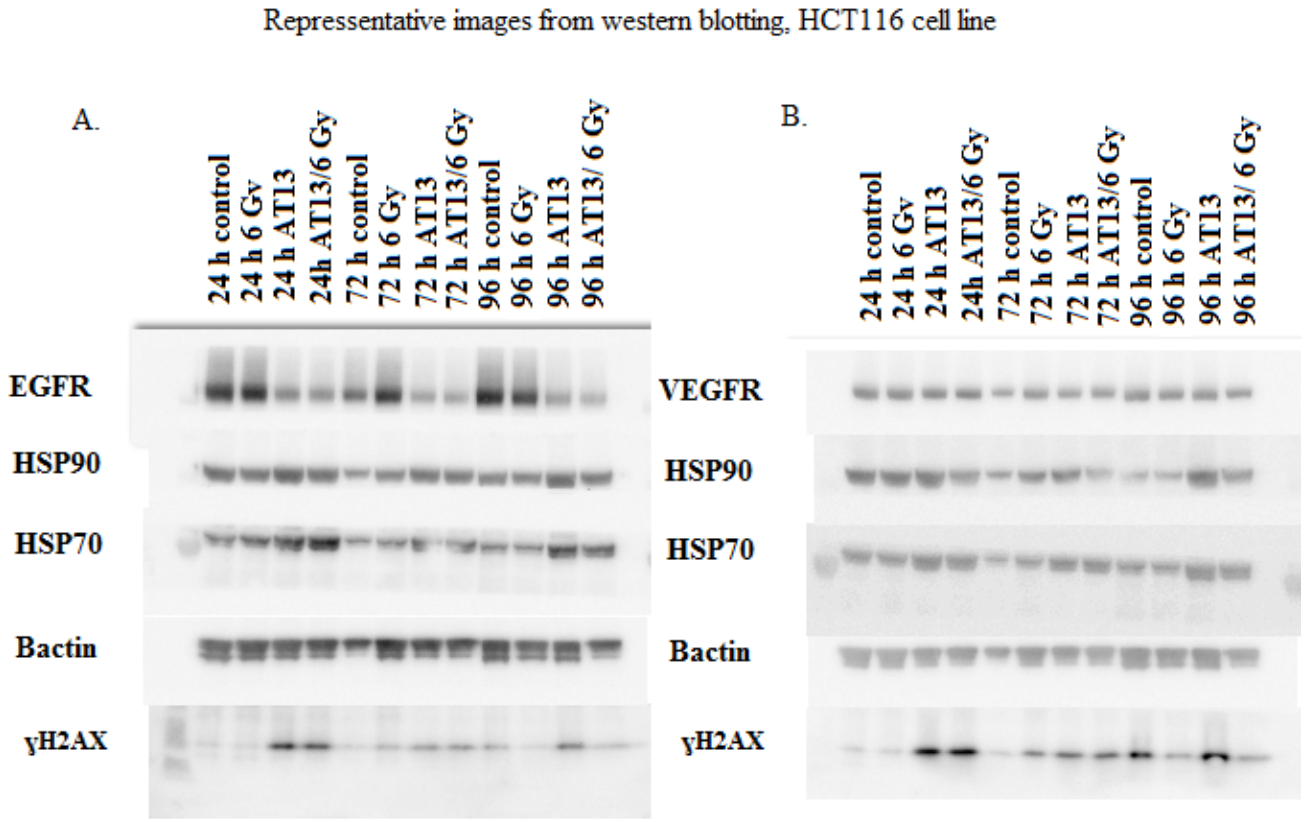

Figure 19: A. Representative image of the results from western blotting for the HCT116 cell line. ß-ACTIN is used as a control protein. Proteins investigated in this assay were EGFR, HSP90, HSP70 and ɣH2AX. **B**. One more representative image of the results from western blotting for the HCT116 cell line. The difference from A is that here the expression of VEGFR is investigated instead of EGFR.

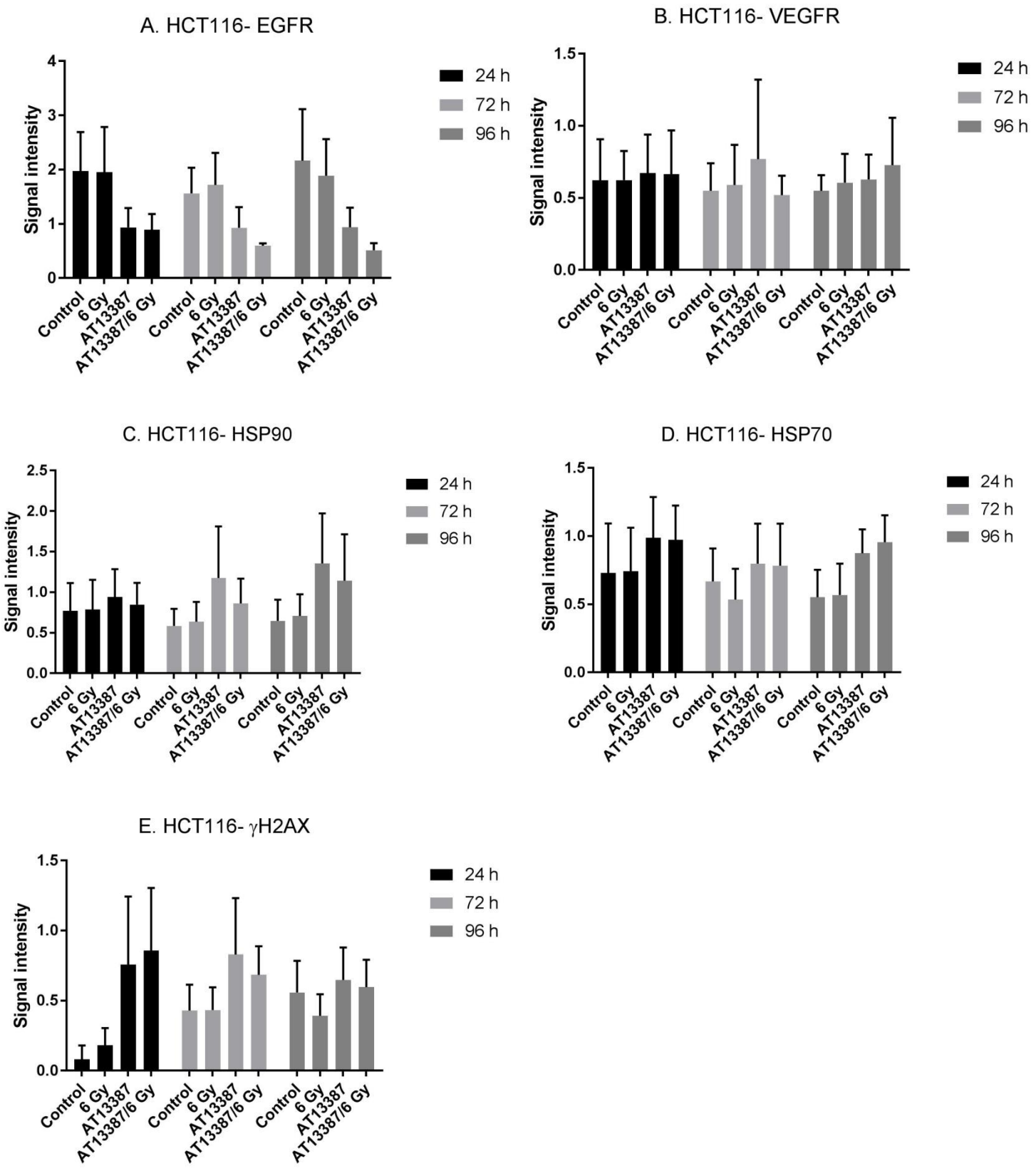

Figure 20: All the figures represents graphs translated from figure 19 using the program ImageJ. **A**. Demonstrate how EGFR varies through the different treatments and after different time points. In all the time points, EGFR is highly down regulated after treatments with AT13387 and AT13387 and irradiation, respectively (n=3, error bars= SD). **B**. Showing results for VEGFR, the protein stays

relatively stable throughout all the treatments and time points (n=3, error bars = SD). **C**. Represents results for HSP90. In the later points HSP90 is up regulated after treatments with AT13387 with or without irradiation (n=6, error bars = SD). **D**. Is showing results for HSP70, in all time points HSP70 is up regulated after treatments with AT13387 alone and AT13387 combined with irradiation (n=3, error bars = SD). **E**. Demonstrate how ɣH2AX varies throughout the different treatments and time points. In the first and second time point ɣH2AX is highly up regulated after treatments with AT13387 with and without irradiation (n=4, error bars = SD).

4 Discussion and conclusions

During this project the aim has been to examine and characterize AT13387 in combination with gamma radiation in various human cell lines. The goal was to optimize drug administration and reveal mechanisms behind AT13387s possible radiosensitizing effects. The goal has been reached although the results require more investigation. There are several aspects that need to be taken in consideration when analysing these results.

From the XTT assays it is clear that AT13387 alone and in combination with irradiation reduces cell survival in a concentration dependent manner. The cell viability goes down to almost 0 % after treatments with 300 µM AT13387, which gives the information that AT13387 has a strong killing effect on the cells when the concentration is in the micro molar range. When normalizing the data to the untreated controls (100 %) and to cells treated with a radiation dose of 6 Gy (100 %), both curves overlap at almost all concentrations. That means that the effects of both drug and radiation treatment are additive. These results imply that by combining both treatments eventfully more cancer cells could be eradicated more efficiently than by the single treatments. However, synergistic effects where one treatment can potentiate the outcome of another could be even more desirable in cancer patient management. To utilize such effects the concentration and timing of the treatment has to be optimized. A reason why there is no difference between AT13387 alone and AT13387 with irradiation can be that measurements are only taken after 24 h. An explanation can be that the irradiation effect have not reached its' fully effect and a bigger difference would have been observed if measurements would have been taken after a later time point than 24 h. This is something that would be interesting to further investigate.

From the migration assays a trend of a slight difference between the two treatments AT13387 alone and the combination of AT13387 and radiation can be seen. At least for HCT116 cells where the migration capacity is a little more reduced for the combination treatment than for treatment with AT13387 alone, however there is no significant difference between them. The error bars are quite big in these results and that is why it is hard to distinguish how big the difference between the two treatments really is. However, it is very clear that AT13387 with or without irradiation is reducing the migration capacity of the cells. The big error bars might have to do with the assay itself. Although it is a very easy method to perform the results can be unreliable in the sense that if the scratch is too wide cells will not migrate towards each

other. It is important to keep in mind that even though the difference is small between AT13387 alone and AT13387 with irradiation, this small difference can have an effect in patients and that is what is most important.

The biggest indications that AT13387 possesses radiosensitizing effects are results from wide field microscopy and flow cytometry. In the wide field microscopy it is very clear that the combination treatment with AT13387 and irradiation are causing more double strand breaks in the nucleuses than all the other treatments. From flow cytometry, both HSP70 and CASPASE-3 are highly up-regulated for the combination treatment in HCT116 cells. This means that HCT116 cells are more apoptotic after the combination treatment than cells from the other treatments. This is a big indicator of the powerful effect of AT13387 together with irradiation. The up regulation of HSP70 indicates more activity from HSP70 which means that it tries to take over the inhibited HSP90s functions. However, it is surprising that we cannot see an increase of HSP70 or CASPASE-3 for the combination treatment in the 48 h and 72 h samples, respectively. Though an explanation can be that this method relies on a good staining with the primary and secondary antibodies, if something has not been done in exactly the same way, it will show in the result.

Other results that indicate the radiosensitizing effects of AT13387 are results from western blotting. In A431 cells, that are known to be very radioresistant, the DNA damage is biggest in the combination treatment after 24 h. This means that the cells from the combination treatment have the hardest time to recover after exposure of the treatment. This trend can also be seen in HCT116 cells, most of the time in all the time points the combination treatment show the highest indication of DNA damage. The down regulation of EGFR in both cell lines and down regulation of VEGFR in the A431 cell line are indications that AT13387 possesses radiosensitizing effects, since the combination treatments indicate the biggest down regulation. Since both EGFR and VEGFR are known to be involved in cancer and cell survival after irradiation, the down regulation of these two proteins is a success for AT13387 (Spiegelberg *et al.* 2015, Gupta *et al.* 2002). A surprising result from western blotting is the up regulation of HSP90 in both cell lines. This result contradicts what previously have been published about inhibition of HSP90. Previous publications have shown down regulation of HSP90 after treatment with the inhibitor. This surprising result should be further investigated. The up regulation of HSP70 is something to keep in mind for future drug development since experiments from both flow cytometry and western blotting in this project show up regulation of the protein.

AT13387 with irradiation has been examined and characterized through multiple assays in this project. The possible radiosensitizing effects have been examined and results especially from wide field microscopy, flow cytometry and western blotting are results that strengthen the fact that AT13387 possesses radiosensitizing effects. The project has showed that AT13387 with irradiation has effect on tumour cells in the nano molar range. Even though the difference in most cases is little between AT13387 alone and AT13387 with irradiation, it is still a difference and it may have a positive effect for patients. All these results strengthen the

fact that AT13387 is a promising therapeutic drug and more investigation is needed in the combination treatment of AT13387 and irradiation.

5 Future aspects

This project supports the fact that AT13387 is a potent cancer drug and that combination treatment with radiation could be beneficial. Therefore, the combination of AT13387 and radiotherapy should be investigated in a clinical setting. So far, AT13387 has only been tested alone in clinical trials and not with the combination of irradiation. What also could be interesting for future drug development would be a drug that inhibits both HSP90 and HSP70. This, since this project shows that HSP70 is up regulated when HSP90 is inhibited, and might therefore give a better radiosensitizing effect.

Acknowledgements

I would like to thank my supervisor Diana Spiegelberg for all the help and support I have got during this project. It has been great working with you and I have learned a lot! I would also like to thank my scientific reviewer Marika Nestor for the help with this report and for letting me do my master thesis in your group. Finally I would like to say thank you to everyone in both Marika's group and Bo Stenerlöw and his group, thanks for all the help and guidance during my 5 months at Rudbeck laboratory!

References

Ahmed, Eide PW, Eilertsen IA, Danielsen SA, Ekn?s M, Hektoen M, Lind GE, Lothe RA. 2013. Epigenetic and genetic features of 24 colon cancer cell lines. Oncogenesis 2: e71.

Ahsan, Ramanand SG, Whitehead C, Hiniker SM, Rehemtulla A, Pratt WB, Jolly S, Gouveia C, Truong K, Waes CV, Ray D, Lawrence TS, Nyati MK. 2012. Wild-type EGFR Is Stabilized by Direct Interaction with HSP90 in Cancer Cells and Tumors. Neoplasia 14: 670-IN1. 2013. Epigenetic and genetic features of 24 colon cancer cell lines. Oncogenesis 2: e71.

Alegria-Schaffer, Lodge A, Vattem K. 2009. Chapter 33 Performing and Optimizing Western Blots with an Emphasis on Chemiluminescent Detection. Methods in Enzymology, pp. 573–599. Elsevier

Brown, Wittwer C. 2000. Flow cytometry: principles and clinical applications in hematology. Clinical Chemistry 46: 1221–1229.

Chiosis, Vilenchik M, Kim J, Solit D. 2004. Hsp90: the vulnerable chaperone. Drug Discovery Today 9: 881–888.

Gupta, Jaskowiak NT, Beckett MA, Mauceri HJ, Grunstein J, Johnson RS, Calvin DA, Nodzenski E, Pejovic M, Kufe DW, Posner MC, Weichselbaum RR. 2002. Vascular endothelial growth factor enhances endothelial cell survival and tumor radioresistance. Cancer Journal (Sudbury, Mass) 8: 47–54.

Gustafsson. 2005. Nonlinear structured-illumination microscopy: Wide-field fluorescence imaging with theoretically unlimited resolution. Proceedings of the National Academy of Sciences 102: 13081–13086.

Hartmann, Wess D, Witte I. 1995. Enhanced cyto- and genotoxicity of tetracycline in Wilson disease fibroblasts. Mutation Research Letters 348: 7–12.

Jemal, Siegel R, Xu J, Ward E. 2010. Cancer Statistics, 2010. CA: A Cancer Journal for Clinicians 60: 277–300.

Kabakov, Kudryavtsev VA, Gabai VL. 2010. Hsp90 inhibitors as promising agents for radiotherapy. Journal of Molecular Medicine 88: 241–247.

Kuo, Yang L-X. 2008. Gamma-H2AX - a novel biomarker for DNA double-strand breaks. In Vivo (Athens, Greece) 22: 305–309.

Liang C-C, Park A.Y, Guan J-L. 2007. In vitro scratch assay: a convenient and inexpensive method for analysis of cell migration in vitro.Nature. doi:10.1038/nprot.2007.30

Murray, Carr MG, Callaghan O, Chessari G, Congreve M, Cowan S, Coyle JE, Downham R, Figueroa E, Frederickson M, Graham B, McMenamin R, O'Brien MA, Patel S, Phillips TR, Williams G, Woodhead AJ, Woolford AJ-A. 2010. Fragment-Based Drug Discovery Applied

to Hsp90. Discovery of Two Lead Series with High Ligand Efficiency. Journal of Medicinal Chemistry 53: 5942–5955.

National cancer institute, https://www.cancer.gov/about-cancer/understanding/what-is-cancer 2017-04.12, received: 2017-07-26

Panier, Boulton SJ. 2013. Double-strand break repair: 53BP1 comes into focus. Nature Reviews Molecular Cell Biology 15: 7–18.

Phan, Moffitt RA, Stokes TH, Liu J, Young AN, Nie S, Wang MD. 2009. Convergence of biomarkers, bioinformatics and nanotechnology for individualized cancer treatment. Trends in Biotechnology 27: 350–358.

Porter, Jänicke RU. 1999. Emerging roles of caspase-3 in apoptosis. Cell Death and Differentiation 6: 99–104.

Shapiro, Kwak E, Dezube BJ, Yule M, Ayrton J, Lyons J, Mahadevan D. 2015. First-in-Human Phase I Dose Escalation Study of a Second-Generation Non-Ansamycin HSP90 Inhibitor, AT13387, in Patients with Advanced Solid Tumors. Clinical Cancer Research 21: 87–97.

Shibuya. 2011. Vascular Endothelial Growth Factor (VEGF) and Its Receptor (VEGFR) Signaling in Angiogenesis: A Crucial Target for Anti- and Pro-Angiogenic Therapies. Genes & Cancer 2: 1097–1105.

Sigma-aldrich, http://www.sigmaaldrich.com/catalog/product/roche/11465015001?lang=en&region=SE, received: 2017-07-26

Solomon, Hagekyriakou J, Trivett MK, Stacker SA, McArthur GA, Cullinane C. 2003. EGFR blockade with ZD1839 (?Iressa?) potentiates the antitumor effects of single and multiple fractions of ionizing radiation in human A431 squamous cell carcinoma. International Journal of Radiation Oncology*Biology*Physics 55: 713–723.

Spiegelberg D, Dascalu A, Mortensen A. C, Abramenkovs A, Kuku G, Nestor M, Stenerlöw B. 2015. The novel HSP90 inhibitor AT13387 potentiates radiation effects in squamous cell carcinoma and adenocarcinoma cells. Oncotarget, doi 10.18632/oncotarget.5363

Stemmer, Beck M, Fiolka R. 2008. Widefield fluorescence microscopy with extended resolution. Histochemistry and Cell Biology 130: 807–817.

Sun, Leaman DW. 2005. Involvement of Noxa in Cellular Apoptotic Responses to Interferon, Double-stranded RNA, and Virus Infection. Journal of Biological Chemistry 280: 15561–15568.

ThermoFisher Scientific, https://www.thermofisher.com/se/en/home/references/protocols/cell-and-tissue-analysis/protocols/xtt-cell-viability-assay-protocol.html, received: 2017-07-26

Torre, Bray F, Siegel RL, Ferlay J, Lortet-Tieulent J, Jemal A. 2015. Global cancer statistics, 2012: Global Cancer Statistics, 2012. CA: A Cancer Journal for Clinicians 65: 87–108.

Trepel, Mollapour M, Giaccone G, Neckers L. 2010. Targeting the dynamic HSP90 complex in cancer. Nature Reviews Cancer 10: 537–549.

Wagner, Agulnik M, Heinrich MC, Mahadevan D, Riedel RF, von Mehren M, Trent J, Demetri GD, Corless CL, Yule M, Lyons JF, Oganesian A, Keer H. 2016. Dose-escalation study of a second-generation non-ansamycin HSP90 inhibitor, onalespib (AT13387), in combination with imatinib in patients with metastatic gastrointestinal stromal tumour. European Journal of Cancer 61: 94–101.

Whitesell, Lindquist SL. 2005. HSP90 and the chaperoning of cancer. Nature Reviews Cancer 5: 761–772.

Woodhead, Angove H, Carr MG, Chessari G, Congreve M, Coyle JE, Cosme J, Graham B, Day PJ, Downham R, Fazal L, Feltell R, Figueroa E, Frederickson M, Lewis J, McMenamin R, Murray CW, O'Brien MA, Parra L, Patel S, Phillips T, Rees DC, Rich S, Smith D-M, Trewartha G, Vinkovic M, Williams B, Woolford AJ-A. 2010. Discovery of (2,4-Dihydroxy-5-isopropylphenyl)-[5-(4-methylpiperazin-1-ylmethyl)-1,3-dihydroisoindol-2-yl]methanone (AT13387), a Novel Inhibitor of the Molecular Chaperone Hsp90 by Fragment Based Drug Design. Journal of Medicinal Chemistry 53: 5956–5969.